Silesian University of Technology

FACULTY OF CHEMISTRY
DEPARTMENT OF PHYSICAL CHEMISTRY AND TECHNOLOGY OF POLYMERS

Shadi Keihankhadiv, M.Sc.

DOCTORAL DISSERTATION

Synthesis and characterization of dual bioactive polymer systems based on choline ionic liquids functionalized with pharmaceutical anions for combined therapy

A Guide to the Monothematic Publication Cycle

Supervisor: Prof. Dorota Neugebauer, PhD. Eng.

Scientific discipline: Chemical Sciences

Gliwice, Poland, 2025

Author:
Shadi Keihankhadiv, M.Sc.
Silesian University of Technology
Faculty of Chemistry
Department of Physical Chemistry and Technology of Polymers
Ul. 9 Strzody Street., Lab.16, 44-100 Gliwice, Poland
E-mail: shadi.keihankhadiv@polsl.pl

Supervisor:
Prof. dr. hab. inż. Dorota Neugebauer
Professor at Silesian University of Technology
Faculty of Chemistry
Department of Physical Chemistry and Technology of Polymers
Ul. 9 Strzody Street., Room 105, 44-100 Gliwice, Poland
E-mail: dorota.neugebauer@polsl.pl

Polish Title:
Synteza i charakterystyka podwójnie bioaktywnych systemów polimerowych opartych na cholinowych cieczach jonowych funkcjonalizowanych anionami farmaceutycznymi do terapii skojarzonej

Acknowledgments

First and foremost, I would like to express my sincere gratitude to my dear supervisor, Prof. Dorota Neugebauer, for her invaluable support, scientific supervision, and guidance throughout this research journey. Her extensive knowledge and experience, along with her patience, understanding, and unwavering commitment, have been fundamental to my progress. I am especially thankful for her kindness and the generous time she dedicated, as well as for her encouragement at each step, which continually motivated me to achieve my goals.

I extend my heartfelt thanks to the dedicated employees and fellow PhD students in our team for their invaluable assistance and for fostering a friendly atmosphere.

Above all, I am profoundly grateful to my family for their constant support, care, and belief in me, which have been a source of strength throughout this endeavor.

Finally, I would like to thank the Silesian University of Technology for providing the scholarship that made this research possible.

ABSTRACT OF DOCTORAL DISSERTATION

This work presents the synthesis and characteristics of novel polymeric carriers in drug delivery systems for antibacterial treatments, including tuberculosis therapy. The systems of linear copolymers were developed using monomeric ionic liquid (MILs) on the base of choline, which was biofunctionalized by incorporation of therapeutic substances.

Preparation of therapeutically active choline monomer was achieved by exchange of the chloride anion in the quaternary ammonium group in the initial [2–(methacryloyloxy)ethyl]trimethylammonium chloride (TMAMA/Cl) on the pharmaceutical anion, including *p*–aminosalicylate (PAS), ampicillin, and cloxacillin. Afterwards, the modified choline monomer was copolymerized with methyl methacrylate (MMA) through controlled atom transfer radical polymerization (ATRP) to generate the well-defined conjugates of linear copolymers functioning as single drug systems. In analogical way, the copolymerization of two pharmaceutically functionalized monomers MIL1 and MIL2 resulted in the dual drug copolymer conjugate systems. This approach enabled the development of various drug delivery systems with tailored compositions.

Furthermore, the amphiphilic properties of choline-based poly(ionic liquid)s (PILs) containing Cl or PAS anions have been confirmed by critical micellization concentration (CMC), demonstrating their suitability as matrices for micellar systems. The unique copolymer structure promoted the formation of self-assembled systems, allowing for the encapsulation of drug, e.g., *p*–aminosalicylate in the form of acidic and sodium salt (PASA, PASNa), and isoniazid (ISO). The encapsulation of drug in the case of Cl-based choline copolymers provided a single drug systems, whereas the ionic conjugates of polymers containing PAS anions were developed to the dual-drug systems with synergistic therapeutic effects (PAS^-/ISO) or to the single-drug systems with enhanced drug efficacy (PAS^-/PASA, PAS^-/PASNa).

In vitro studies confirmed the controlled release of drugs, with initial rapid release observed within the first four hours, followed by a sustained release over 24–72 hours. The structure of the copolymers and the nature of the incorporated drugs influenced the release kinetic profiles. The designed choline-based polymer systems demonstrated strong drug-loading capacities and effective encapsulation, highlighting their potential as advanced carriers for antibacterial therapy.

ABSTRAKT ROZPRAWY DOKTORSKIEJ

Niniejsza praca przedstawia syntezę i charakterystykę nowatorskich nośników polimerowych w układach dostarczania leków do terapii przeciwbakteryjnych, w tym leczenia gruźlicy. Układy kopolimerów liniowych zostały otrzymane z wykorzystaniem monomerycznej cieczy jonowej (MIL) na bazie choliny, którą poddano biofunkcjonalizacji poprzez wprowadzenie substancji terapeutycznej.

Przygotowanie terapeutycznie aktywnego monomeru cholinowego polegało na wymianie anionu chlorkowego w grupie amoniowej wyjściowego chlorku [2–(metakryloiloksy)etylo]–trimetyloamoniowego (TMAMA/Cl) na anion farmaceutyczny, taki jak *p*–aminosalicylanu (PAS), ampicyliny i kloksacyliny. Następnie, zmodyfikowany monomer cholinowy został poddany kopolimeryzacji z metakrylanem metylu (MMA) metodą kontrolowanej polimeryzacji rodnikowej z przeniesieniem atomu (ATRP) w celu uzyskania dobrze zdefiniowanych jonowych koniugatów liniowych polimerów działających jako systemy dostarczające jeden lek. Analogicznie, kopolimeryzacja dwóch farmaceutycznie funkcjonalizowanych monomerów MIL1 i MIL2 prowadziła do powstania koniugatów polimerowych zawierających dwa różne leki w układzie. Podejście to umożliwiło opracowanie różnorodnych systemów dostarczania leków o precyzyjnie dostosowanym składzie.

Ponadto, amfifilowe właściwości cholinowych poli(cieczy jonowych) (PIL) zawierających aniony Cl lub PAS zostały potwierdzone poprzez pomiary krytycznego stężenia micelizacji (CMC), co wykazało ich przydatność jako matryc dla układów micelarnych. Unikalna struktura kopolimerów sprzyjała samoorganizacji umożliwiając enkapsulację leków, tj. PAS w formie kwasowej lub soli sodowej (PASA, PASNa) oraz izoniazydu (ISO). W przypadku kopolimerów zawierających jednostki choliny w przeciwjonem chlorkowym enkapsulacja prowadziła do układów transportujących jeden lek. Z kolei, enkapsulacja leków w matrycy koniugatu polimeru z anionami farmaceutycznymi umożliwiła przygotowanie układów z dwoma lekami o synergistycznym działaniu terapeutycznym (PAS^-/ISO) lub układów z jednym lekiem o zwiększonej skuteczności terapeutycznej (PAS^-/PASA, PAS^-/PASNa).

Badania *in vitro* potwierdziły kontrolowane uwalnianie substancji farmaceutycznych, początkowo szybko uwalnianych w ciągu pierwszych czterech godzin, a następnie stopniowo w ciągu 24–72 godzin. Struktura kopolimerów oraz natura zawartych leków miały istotny wpływ na profile kinetyczne uwalniania. Otrzymane układy polimerów cholinowych wykazały wysoką zdolność do załadowania lekiem oraz skuteczną enkapsulację, podkreślając ich potencjał jako zaawansowanych nośników do terapii przeciwbakteryjnej.

Table of Contents

LIST OF SCIENTIFIC PUBLICATIONS CONSTITUTING A MONOTHEMATIC CYCLE

The dissertation consists of five monothematic scientific papers, detailed below, which were published in journals indexed in the Journal Citation Reports (JCR) database between 2021 and 2024. In the thesis, these papers are cited using abbreviated identifiers (P).

P.1. Synthesis and characterization of linear copolymers based on pharmaceutically functionalized monomeric choline ionic liquid for delivery of *p*–aminosalicylate.
Keihankhadiv, S., & Neugebauer, D.
Pharmaceutics. **2023**, *15*(3), p.860. (IF_{2022}=5.4; MEiN= 140pkt)

P.2. Self-assembling polymers with *p*–aminosalicylate anions supported by encapsulation of *p*–aminosalicylate for the improvement of drug content and release efficiency.
Keihankhadiv, S., & Neugebauer, D.
Pharmaceuticals, **2023**, *16*(10), p.1502. (IF_{2022}= 4.67; MEiN= 140 pkt)

P.3. Ionic liquid-based polymer matrices for single and dual drug delivery: impact of structural topology on characteristics and in vitro delivery efficiency.
Niesyto, K., Keihankhadiv, S., Mazur, A., Mielańczyk, A. and Neugebauer, D.
International Journal of Molecular Sciences, **2024**, *25*(2), p.1292. (IF_{2022}=5.6; MEiN=140 pkt)

P.4. Simple strategy of the use of pharmaceutically functionalized ionic liquids in a new generation of polymer nanocarriers for the combined delivery of ionic *p*–aminosalicylate and ampicillin.
Keihankhadiv, S., & Neugebauer, D.
International Journal of Pharmaceutics, **2024**, *662*, p.124483. (IF_{2022}=5.8; MEiN=100 pkt, CS-hp2023=92)

P.5. Polymerizable cholinium-based antibiotics for polymer carriers: systems with combined load of cloxacillin and ampicillin.
Keihankhadiv, S., & Neugebauer, D.
Molecules, **2024**, *29*(24*)*, p.5973. (IF_{2023}=4.2; MEiN=140 pkt, CS-hp2023=83)

Statements from co-authors detailing their individual authorial contributions to these publications are provided in the appendices of this dissertation.

LIST OF ABBREVIATIONS USED

ARD	Amount of released drug
ATRP	Atom transfer radical polymerization
AMP	Ampicillin
AMPNa	Ampicillin sodium salt
CMC	Critical micelle concentration
CuBr	Copper bromide
CLX	Cloxacillin
CLXNa	Cloxacillin sodium salt
Cl	Chloride anion
DC	Drug content
DLC	Drug loading content
DDS	Drug delivery system
DLS	Dynamic Light Scattering
Dh	Hydrodynamic diameters
DMSO-d6	Deuterated dimethyl sulfoxide
DP_n	Degree of polymerization
DP_{M1}	Degree of polymerization of the ionic monomers
Đ	Dispersity index
EBiB	Ethyl 2-bromoisobutyrate
F_{M1}	Content of ionic fraction in the copolymer
f_{M1}/f_{M2}	Initial content of monomer in the reaction mixture (initial comonomer ratios)
^{1}H-NMR	Proton nuclear magnetic resonance
HPMA	*N*-(2-hydroxypropyl)methacrylamide
ISO	Isoniazid
IL	Ionic liquid
MeOH	Methanol
MIL	Monomeric ionic liquid
MMA	Methyl methacrylate
M_n	Average molecular weight of polymer
Mn_{SEC}	Average molecular weight of polymer determined by size-exclusion chromatography
Mn_{NMR}	Average molecular weight of polymer determined by proton nuclear magnetic resonance
PASNa	*p*-Aminosalicylate sodium salt
PAS	*p*-Aminosalicylate
PASA	*p*-Aminosalicylate acid
PBS	Phosphate buffer saline
PDI	Polydispersity index
PEO/PEG	Poly(ethylene oxide)/polyethylene glycol
PIL	Poly(ionic liquid) / polymerized ionic liquid
PMDETA	*N*,*N*,*N*′,*N*″,*N*″–pentamethyldiethylenetriamine
SEC	Size exclusion chromatography
THF	Tetrahydrofuran
TMAMA/AMP	[2–(methacryloyloxy)ethyl]trimethylammonium ampicillin
TMAMA/PAS	[2–(methacryloyloxy)ethyl]trimethylammonium *p*-aminosalicylate

TMAMA/CLX	[2–(methacryloyloxy)ethyl]trimethylammonium cloxacillin
TMAMA/Cl	[2–(methacryloyloxy)ethyl]trimethylammonium chloride
TMAMA/X	[2–(methacryloyloxy)ethyl]trimethylammonium pharmaceutical
TB	Tuberculosis
WCA	Water contact angle
UV-Vis	Ultraviolet-visible light spectroscopy
X	Total conversion of comonomers
X_{M1}	TMAMA monomer conversion
X^-	pharmaceutical anion

1. PURPOSE AND SCOPE OF RESEARCH

The objective of the research presented in this doctoral dissertation was to develop novel polymer systems to serve as drug carriers based on bioactive linear poly(ionic liquid)s (PILs) for either single or dual drug delivery applications. These carriers were synthesized with the use of a monomeric ionic liquid (MIL) containing a pharmaceutical anion, which enabled the creation of therapeutically functionalized monomers for controlled atom transfer radical polymerization (ATRP). For this purpose, the chloride counterions in the quaternary ammonium groups of the choline-based MIL, such as [2–(methacryloyloxy)ethyl]trimethylammonium chloride (TMAMA/Cl), underwent anion exchange with a sodium salt of the selected pharmaceuticals, thus introducing a functional anion with distinct therapeutic properties.

In the first series of ATRP reactions, the modified choline monomer was copolymerized with methyl methacrylate (MMA) to produce well-defined linear copolymers as single drug systems with various content of TMAMA and pharmaceutical anions, controlled by adjusting the initial TMAMA–to–MMA ratio. In the second series of ATRP reactions, performed under the same conditions, two pharmaceutically functionalized MILs were copolymerized with MMA to create dual drug polymer conjugates.

A second major focus of this research was to utilize the amphiphilic nature of the copolymers for the encapsulation of selected drugs, thereby forming micellar systems for both single and dual drug delivery. By combining anion exchange on the monomers before polymerization and drug encapsulation after polymerization in linear copolymer conjugates, the dual drug micellar systems were developed as platforms for combination therapies.

Both types of dual systems transported two drugs with synergistic effects, interacting differently with the polymer matrix, that is through ionic binding or physical encapsulation. Comprehensive *in vitro* drug release studies were investigated by comparison of kinetics profiles for various choline-based polymer systems to find correlation between their structural parameters and delivery properties, which let to define the most efficient polymer carriers for DDS.

The conducted research consists of the following tasks:

Ion Exchange: The Cl counterion in the choline-based monomeric ionic liquid was exchanged with a pharmaceutical anion by sodium salt of *p*–aminosalicylate (PAS), ampicillin (AMP), cloxacillin (CLX) to produce a modified monomer.

1. **Synthesis of Well-Defined Linear Copolymer Conjugates via ATRP** using:
    - unmodified choline monomer containing Cl anions (TMAMA/Cl),
    - one modified choline monomer, such as TMAMA/PAS, TMAMA/AMP and TMAMA/CLX, to get single drug systems,
    - two modified choline monomers, such as (TMAMA/PAS with TMAMA/AMP) and (TMAMA/AMP with TMAMA/CLX), to get dual drug systems.
2. **Standard physicochemical characteristics:**
    - monomers by proton nuclear magnetic resonance (^{1}H–NMR) spectroscopy to verify the chemical structure of the MILs, including the introduction of pharmaceutical anions through anion exchange.
    - polymers by ^{1}H–NMR spectroscopy and size exclusion chromatography (SEC) to confirm well-defined and precise structures.
3. **Micellization and Encapsulation**: Linear copolymer conjugates containing Cl anions P(TMAMA/Cl–*co*–MMA)s, or single drug systems containing PAS anions P(TMAMA/PAS–*co*–MMA)s, were self-assembled and encapsulated with *p*-aminosalicylate sodium (PASNa), *p*-aminosalicylic acid (PASA) and isoniazid (ISO) to obtain micellar systems as single and dual drug systems.
4. **Monitoring Drug Release**: The drug release studies of polymer conjugates (containing PAS, AMP, CLX, PAS/AMP, AMP/CLX) and micellar systems with encapsulated drugs (PASNa, PASA, ISO, PAS/PASNa, PAS/PASA, PAS/ISO) were conducted in phosphate-buffered saline (PBS) at pH 7.4 simulating physiological conditions over a 72–hour period and assessed using UV–Vis spectroscopy.

2. INTRODUCTION

Over the last two decades, various drug delivery systems (DDS) have been explored to enhance the bioavailability and administration of pharmaceuticals [1, 2, 3, 4]. Conventional drug delivery methods such as normal tablets and capsules often encounter challenges such as rapid drug degradation, poor solubility, and uncontrolled release, which can result in suboptimal therapeutic outcomes and potential toxicity from high drug concentrations [5, 6]. These limitations reduce the efficacy of pharmaceuticals and pose risks to healthy tissues [7, 8, 9, 10].

2.1. NANOCARRIERS IN DRUG DELIVERY SYSTEMS

To address these challenges, nanocarriers have emerged as highly promising innovations in advanced DDS [11, 12, 13, 14, 15]. They can improve the solubility and stability of poorly soluble drugs and provide targeted delivery and enhance absorption of drug in a specific tissues, for instance tumor [16, 17, 18, 19, 20, 21]. Additionally, they can navigate biological barriers, such as the blood–brain barrier, protecting drugs from premature degradation with the biological environment and extending their circulation time [22, 23, 24]. By enabling precise control over drug release, they can sustain therapeutic levels in the bloodstream, thereby decreasing the frequency of dosing [22, 25]. The improved control over drug pharmacokinetics and biodistribution lead to better therapeutic outcomes [26]. Among the advanced approaches, stimulus-responsive carriers represent a cutting-edge innovation in nanocarrier technology. These systems are engineered to respond to specific internal or external triggers, such as temperature changes, pH variations, light exposure, magnetic fields, or specific biological molecules [27, 28, 29, 30, 31]. They are particularly advantageous in treating complex conditions, such as cancer, where precise targeting and controlled drug release are essential. These advanced systems can dynamically adjust drug release profiles in response to the target environment, allowing real-time adaptation to the changing conditions. This capability not only enhances treatment effectiveness but also reduces the risk of drug resistance and toxicity, addressing challenges that traditional drug delivery methods cannot overcome [32].

2.1.1. POLYMER-BASED NANOCARRIERS

Polymer-based nanocarriers play a crucial role in advanced DDS due to their structural versatility and ability to respond to physiological stimuli [33, 34, 35, 36, 37, 38], drug encapsulation and release in a controlled manner [39, 40, 41]. The precise synthesis of polymers with precise architectures, defined compositions, uniform chain lengths, and site-specific functionalities [42, 43, 44, 45], such as mechanical strength, bioactivity, tissue adhesiveness, biodegradability and processability [46, 47], creating custom-made polymers through controlled polymerization methods [48, 49, 50, 51]. These engineered polymer structures, such as linear, star-shaped [52, 53, 54] and grafted topologies [55, 56, 57] with bio-therapeutics functions [58, 59, 60], enable the design of nanoparticles with varied shapes, sizes, and surfaces that improve targeting, prolonging release times and intracellular delivery to organelles like endosomes, lysosomes, and the cytoplasm [61]. Their optional biodegradability allows them to decompose safely after completing their therapeutic role, reducing long-term toxicity risks [62]. Polymers with ionizable groups, such as polyethylenimine (PEI), are particularly effective for intracellular drug delivery due to their ability to destabilize endosomal membranes through the "proton sponge effect," which facilitates the release of drugs into the cytoplasm [63, 64, 65]. Polymer carriers are utilized to deliver targeting moieties such as antibodies [66], ligands [67, 68], as well as imaging agents like contrast dyes, fluorescent markers, and radioactive tracers, which enhance visualization in techniques like magnetic resonance imaging (MRI), and fluorescence imaging [69, 70]. Additionally, they transport proteins, such as enzymes [71, 72], and therapeutic peptides to protect them from degradation and enhance therapeutic effectiveness [73, 74, 75, 76]. Various polymer-based DDS have been developed, such as polymer-drug conjugates [53, 77, 78, 79], hydrogels [80], nanoparticles [81], dendrimers [82, 83], liposomes [84], capsules [85], cross-linked microgels/nanogels [86, 87], micelles [88, 89, 90] and vesicles [91], allowing drugs to be either conjugated with polymers or encapsulated within polymer nanostructures. Each type offers distinct properties tailored to specific therapeutic needs; hydrogels provide sustained release in localized tissues [92], and nanoparticles enable targeted delivery, significantly improving the overall efficiency and effectiveness of drug administration [93]. Extensive research has focused on both polymer-based encapsulation

(polymeric micelles) and polymer-drug conjugation to overcome issues with drug hydrophilicity [94, 95].

2.1.2. POLYMERIC MICELLES

Polymeric micelles have gained significant attention in the past decade as versatile and effective nanocarriers in DDS [96, 97, 98]. They are formed through the self-assembly of amphiphilic polymers involving hydrophobic and hydrophilic phase segregation [99, 100, 101]. The self-organization process that occur when the concentration of amphiphilic polymer, including linear and graft copolymers [102, 103], exceeds a particular threshold referred to as the critical aggregation concentration (CAC) or critical micelle concentration (CMC) [104, 105, 106, 107, 108, 109]. At this point, in aqueous environment the hydrophobic segments of the block copolymers aggregate to reduce their exposure to water molecules, resulting in the creation of a vesicular or core-shell micellar structure (monolayers) [110, 111, 112, 113, 114, 115, 116], differ from vesicles, which are bilayers of self-assembled polymers [117, 118, 119, 120, 121]. A lower CMC correlates with more stable micelles under physiological conditions [122], essential for their effectiveness as drug delivery vehicles [64, 123, 124, 125]. The sizes of the micelles are in the range of 10 to 100 nm. The micelles morphology depends on the balance between hydrophobic and hydrophilic segments and the solvent conditions yielding spherical, tubular, and inverse micelles, as well as bottle shaped structures that are developed for various applications [107]. Various methods are used to prepare micelles, including dilution [107, 126, 127], lyophilization [127, 128], solvent evaporation [129, 130, 131], dialysis [129, 132, 133], and oil–in–water emulsion [134]. They are characterized by multiple techniques, such as dynamic light scattering (DLS), small–angle X–ray scattering (SAXS), small-angle neutron scattering (SANS), electron paramagnetic resonance (EPR) spectroscopy, transmission electron microscopy (TEM), and atomic force microscopy (AFM) [133].

Moreover, the simultaneous delivery of various bioactive compounds has been investigated to improve the effectiveness of the main drug [135, 136, 137]. Polymeric micelles are particularly notable for their ability to co-deliver multiple drugs, for example doxorubicin (DOX) and paclitaxel, providing an effective strategy for targeting multidrug-resistant tumors. Notably, the representative block copolymers are self-assembled into micelles characterized by a hydrophilic poly(ethylene oxide) (PEO) shell, which enhances their stability in the bloodstream, and a hydrophobic core made of

poly(L–amino acids) segments, which is suitable for encapsulating hydrophobic drugs. This structure shows significant potential in improving the delivery and efficacy of hydrophobic anticancer drugs through passive tumor targeting due to the enhanced permeability and retention effect [138].

2.1.3. POLYMER-DRUG CONJUGATES

Polymer–drug conjugates, initially introduced by Horst Jatzkewitz in 1955, serve as an innovative delivery system for the drug [139]. In 1975, Helmut Ringsdorf established the conceptual framework for their use as targeted drug carriers [140]. Since that pivotal development, the field has made significant advancements, particularly in clinical trials [141]. This system is characterized by a strategically designed covalent bond that links a water–soluble polymer to a bioactive molecule via bioresponsive linkers, enhancing stability while maintaining the diversity, specificity, and functionality of biomolecules [142]. Polymer carrier can improve drug solubility and loading capacity [143], as well as control pharmacokinetic profiles by efficient drug release [144, 145], and enhance drug half-life by decreasing immune system recognition. Additionally, they increase drug accumulation specificity at the target site through passive and active transport mechanisms [146, 147, 148, 149]. The development of new polymer drug conjugates that effectively interact with biological systems remains a challenge, as the drugs need to possess free functional groups that allow direct conjugation to polymer backbones through chemical linkers. The macromolecular conjugates facilitate the simultaneous delivery of drugs and/or bioactive molecules with varying properties, functioning as multifunctional nanocarriers [150, 151]. Due to these benefits, polymer drug conjugates have been applied extensively in medicinal treatments for various diseases, such as cancer, osteoporosis, infection, and immunodeficiency. A wide variety of polymeric carriers have been explored for drug conjugation, with polyethylene glycol (PEG) and polymers of *N*–(2–hydroxypropyl)methacrylamide (PHPMA) being among the most studied [152, 153]. Notably, PEGylated protein, that is bovine–serum–albumin–conjugated PEG, has shown significant application in disease treatment [154, 155], while PHPMA–DOX polymer-drug conjugates have demonstrated enhanced anticancer efficacy with reduced side effects, advancing to clinical trial [156, 157, 158]. To date, several PEG-drug conjugates have received approval of food and drug administration (FDA) [159, 160]. In conclusion, the combination of biocompatibility, structural support,

and modifiable surfaces has made polymer nanocarriers a cornerstone in clinical applications [161], with approved treatments for various diseases including anticancer therapy, tumor targeted immunotherapy, modern vaccines, respiratory infections, diabetes, inflammatory disorders and regenerative medicine [162, 163, 164, 165].

2.2. IONIC LIQUIDS

One specific group of amphiphilic copolymers is derived from ionic liquids (ILs) used as monomers (MIL). ILs are a distinctive class of liquid salts composed of organic cations and anions [166, 167, 168, 169]. They possess melting points below 100°C and are non-flammable, stable thermally and chemically with low vapor pressure at room temperature and adjustable viscosities, chemically inert with tunable polarity, and represent high ionic conductivity [170, 171, 172, 173, 174, 175]. These properties, along with the ability to undergo ionic exchange, make ILs highly versatile and customizable, allowing for the modification of their physicochemical properties [176, 177]. Due to these tunable properties, ILs have found widespread applications in various fields, including synthesis, catalysis, extraction, electrochemistry, analytics, and biotechnology [178, 179]. Their ability to alter properties through ion exchange makes them particularly attractive for ecological, biochemical, and medical applications [180, 181].

Among the bioactive ILs, choline-based ILs are particularly noteworthy due to their biocompatibility, bioavailability and inherent biological activity [182]. Choline, identified as 2–hydroxyethyl trimethylammonium chloride, is a naturally occurring compound produced by the human body through hepatic synthesis, where it plays vitamin-like functions. It is employed in a variety of vital processes as a part of phospholipids such as phosphatidylcholine (lecithin) and as a precursor to acetylcholine, a vital neurotransmitter. Choline–based ILs can demonstrate antibacterial [183, 184], anti-inflammatory and antioxidant activities which is particularly advantageous in biomedical applications [185]. Additionally, their ionic structure facilitates ion exchange between chloride anions and pharmaceutical anions, either before or after polymerization. This adaptability enables choline–based IL units in polymeric carriers to enhance the pharmacodynamic and pharmacokinetic of carried drugs, offering promising alternatives to traditional pharmaceutical formulations [186]. Their biological attributes include enhancing skin penetration [187], functioning as stabilizers [188, 189], cytotoxic and local anesthetic properties, anti-fungal and anti-acne activities, and antibiotic actions [177, 190, 191].

Generally, the versatility of IL drugs, extends to their role in accommodating a wide range of pharmaceutical substances, including antiviral, antimicrobial, antioxidant, anticoagulant, nonsteroidal anti–inflammatory drugs, anticancer agents, and others [177, 192, 193, 194, 195, 196, 197]. The widely employed cholinium cation offers biodegradability, water–solubility, and low cost for various applications [182, 198, 199]. These bioactive ILs have been studied in combination with various drugs, such as phenytoin [200], ampicillin (AMP) [201], nalidixic acid, and niflumic acid, *p*–aminosalicylic acid (PASA), pyrazinoic acid, and picolinic acid demonstrating enhanced solubility and increased membrane permeability of active pharmaceutical ingredients [182, 198].

2.2.1. POLYMERIZED CHOLINE IONIC LIQUIDS

Specific groups of ionic copolymers, known as poly(ionic liquid)s or polymerized ionic liquids (PILs), are derived from monomeric ionic liquids (MILs) [202]. These copolymers can be synthesized through controlled radical polymerization techniques resulting in the well–defined polymer structures [203]. These polymerized structures, often with chloride counterions, can undergo ion exchange to generate pharmaceutical activities tailored to specific biomedical needs. The commercially available choline ester derivative, [2–(methacryloyloxy)ethyl]trimethylammonium chloride, commonly known as methacryloylcholine (TMAMA/Cl), is a choline–based MILs that plays a crucial role in the synthesis of choline–based PILs [204]. One of the key strategies in enhancing the functionality of choline–based PILs involves ion exchange, where chloride anions in the polymer matrix are exchanged with anionic drugs, such as sulfacetamide [205], *p*-aminosalicylate (PAS) [206, 207], fusidate [206, 208], clavulanate [206, 207], and piperacillin [206, 204]. This ion exchange process allows the PILs to be tailored for specific biomedical applications, generating drug-PIL ionic conjugates with improved pharmacological properties. In addition, the polymerization of choline MILs modified with pharmaceutical anions, such as salicylate [204, 209, 210], fusidate [211], cloxacillin (CLX) [211] has been reported mostly for graft copolymers, whereas the main goal of the presented thesis is related to the linear copolymers to expand the scope of pharmaceutically active choline-based PILs and understand their delivery behavior.

Ionic conjugates have also been synthesized using imidazolium and pyridinium PILs with naproxen anions [212], as well as guanidinium PILs combined with ampicillin

anions [213]. This versatility underscores the potential of PILs as adaptable carriers for diverse pharmaceutical compounds. The capacity to modify PILs by ionic exchange positions them as innovative materials in drug delivery, offering new opportunities for developing pharmaceutically active polymeric systems tailored to specific therapeutic needs.

2.2.2. SELF-ASSEMBLED PILs

Self–assembled PILs have been extensively studied for their ability to form micellar systems that encapsulate and deliver active pharmaceuticals, offering a versatile platform for advanced DDS. The unique amphiphilic nature of PIL–based conjugate enables the creation of micellar structures that not only act as carriers for ionic drugs but also contribute to the overall biological activity of the system by encapsulating a non-ionic second drug into the core of the micelle. This dual functionality makes PIL micelles particularly attractive for combination therapies, where they can co–deliver ionic and non–ionic drugs in one formulation, enhancing the therapeutic efficacy of treatments, especially in cases involving drug-resistant strains. PIL micelles have demonstrated the capability to encapsulate a wide range of active pharmaceuticals, including curcumin [214, 215], paclitaxel [216], DOX [217, 218], dopamine [219], acyclovir [220, 221], rifampicin [208], erythromycin [205], tazobactam [222].

In addition, the systems based on PILs containing pharmaceutical anions and encapsulated with a non-ionic drug in the micellar core, exhibit enhanced overall biological activity, making them highly effective as dual drug delivery platforms [205]. For example, choline-based PILs demonstrated a controlled drug release for micellar conjugate systems with salicylate anions (40–50%) and encapsulated erythromycin (60–70%) over a three-day period [205], or fusidate anions (31–55%) and encapsulated rifampicin (19–31%) [208], and piperacillin anions (21–25 %) and encapsulated tazobactam (47–69%) [222] over a two-day period. These findings underscore the potential of PIL micelles to deliver multiple therapeutics simultaneously, providing a synergistic effect that enhances the treatment's effectiveness.

3. OVERVIEW OF THE RESULTS

As part of this doctoral dissertation, the novel biofunctionalized choline ionic liquid linear copolymers via atom transfer radical polymerization (ATRP) for use in both single and dual delivery systems were designed, synthesized, and characterized. Most of them were prepared utilizing choline–based MILs containing pharmaceutical anion. The amphiphilic nature of these polymer conjugates allowed to self-assemble and encapsulate selected drugs, resulting in the formation of micellar systems. The drugs, including pharmaceutical anions, utilized in this research are aimed at antibacterial treatment, including tuberculosis. Drug release studies were performed in PBS at pH 7.4. An overview of the entire work is presented in Figure 1.

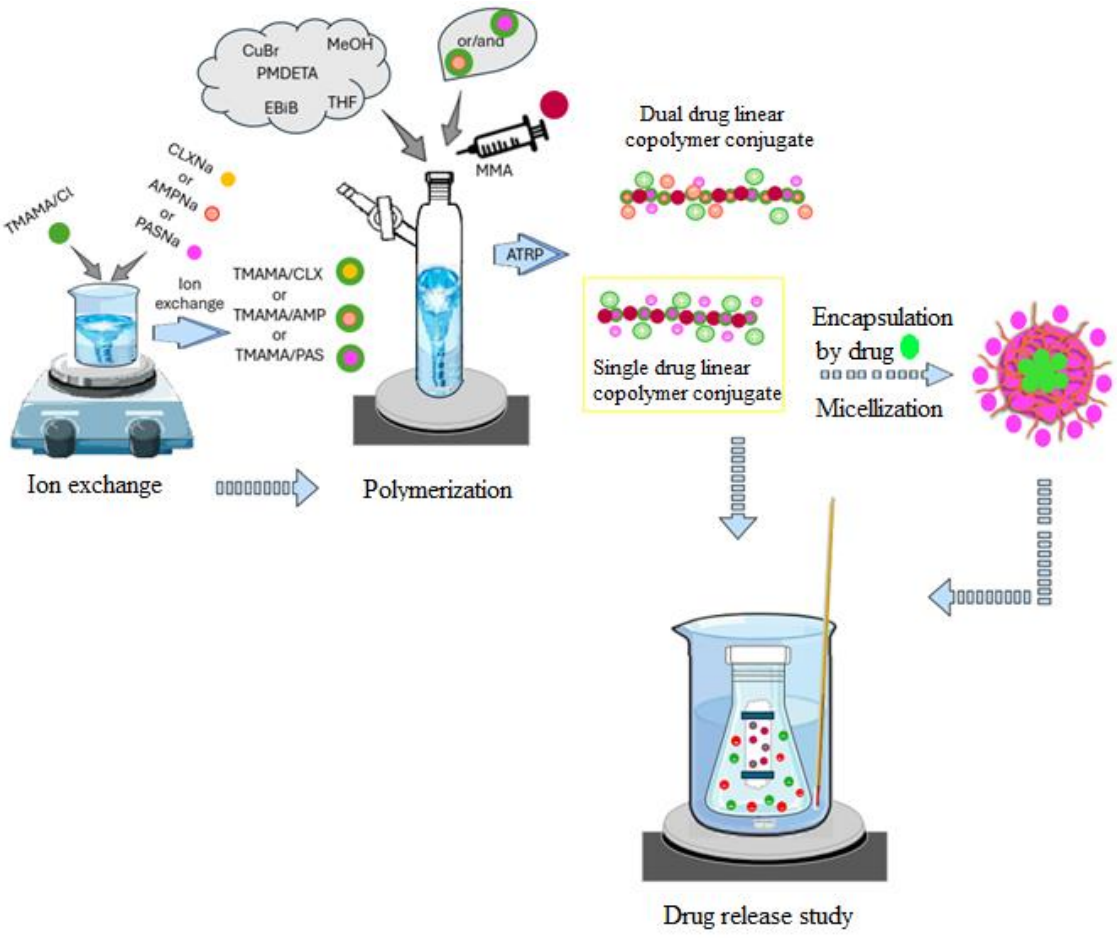

Figure 1. Schematic overview of research studies.

3.1. PREPARATION OF CHOLINE BASED MONOMERIC IONIC LIQUIDS WITH PHARMACEUTICAL ANIONS (P.1.; P.4.; P.5)

Keywords: ionic exchange to TMAMA/PAS (P.1, P.2, P.3, P.4), TMAMA/AMP (P.4, P.5) and TMAMA/CLX (P.5); biological functions of PAS as antituberculosis drug and AMP, CLX as antibiotics; efficiency of drug introduction by ^{1}H-NMR.

The process involved modifying the water-soluble ionic liquid [2–(methacryloyloxy)ethyl]trimethylammonium chloride (TMAMA/Cl), which contains a polymerizable methacrylate group, and quaternary ammonium group with chloride counterion (Cl^{-}), where the letter one was exchanged by pharmaceutical anion (X^{-}), becoming from their sodium salt. This exchange led to the formation of a new monomer containing X^{-}, such as [2–(methacryloyloxy)ethyl]trimethylammonium pharmaceutical (TMAMA/X). The selected drugs for the study included sodium salts of PAS, AMP, and CLX anions. The ion exchange process is illustrated in Figure 2.

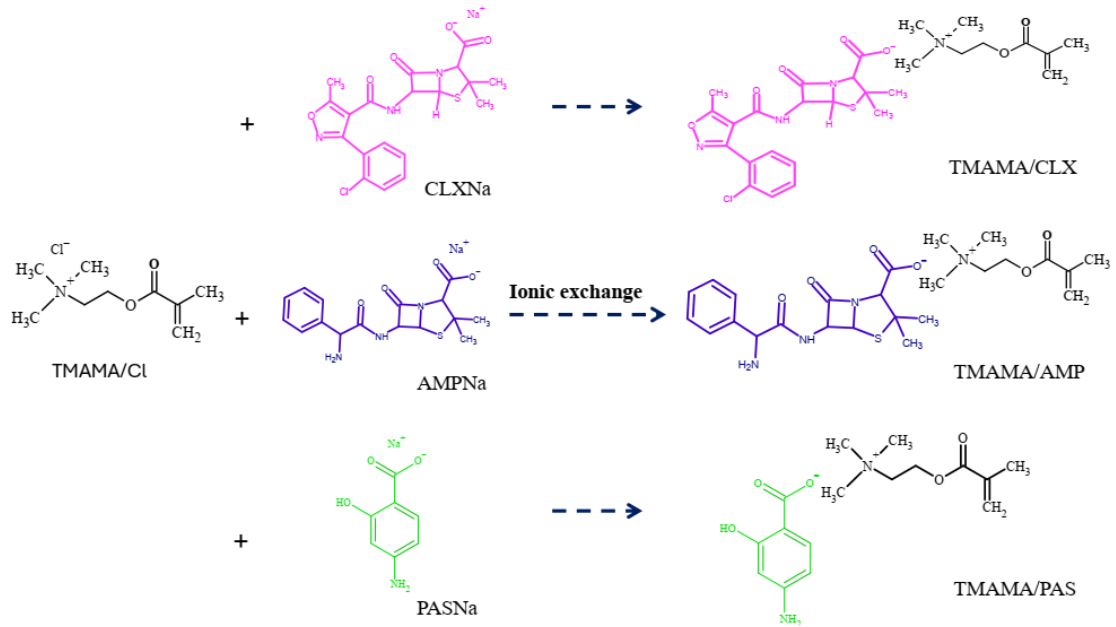

Figure 2. Reaction schemes for ionic exchange of TMAMA/Cl by CLXNa, AMPNa and PASNa to produce TMAMA/CLX, TMAMA/AMP and TMAMA/PAS as the pharmaceutically biofunctionalized MILs.

PAS possesses antibacterial properties and is used in the treatment of tuberculosis [223]. It belongs to the class of drugs known as antitubercular agents. It is effective in inhibiting the growth of *M. tuberculosis* by disrupting folic acid synthesis [224], which is essential for bacterial survival and replication, facilitating their elimination [225]. The chemotherapeutic effect PAS is significantly enhanced through its synergistic interaction with other antitubercular drugs. This interaction not only extends the half-life of these

drugs, allowing them to remain active in the body for longer periods, but also helps prevent the development of drug resistance, a critical concern in tuberculosis treatment. Additionally, PAS has been shown to increase the plasma concentrations of other tuberculosis drugs, such as isoniazid, by competing for the same metabolic pathways [226]. This boosts the overall efficacy of the treatment regimen against *M. tuberculosis* strains, making PAS a valuable component in the management of multi drug resistant tuberculosis [227].

CLX is a β-lactam antibiotic belonging to the penicillinase-resistant penicillin subgroup. It is a semi–synthetic penicillin derivative designed to resist degradation by β–lactamase enzymes, which are produced by certain bacteria to inactivate other penicillin. Chemically, it is known as (2S,5R,6R)–6–[(3–(2–chlorophenyl)–5–methylisoxazole–4–carbonyl)amino]–3,3–dimethyl–7–oxo–4–thia–1–azabicyclo[3.2.0]heptane–2–carboxylic acid. It is effective against gram-positive bacteria and primarily used to treat infections caused by penicillinase–producing *S. aureus*, which are resistant to other penicillin but remain susceptible to CLX due to its ability to withstand enzymatic breakdown [228]. Furthermore, it is indicated for the treatment of a variety of infections, such as skin and skin structure, osteomyelitis, endocarditis and respiratory tract infections and meningitis [229, 230].

AMP is an antibiotic belonging to the β–lactam group and is a semi-synthetic penicillin, chemically known as (2S,5R,6R)–6–([(2R)–2–amino–2–phenylacetyl]-amino)–3,3–dimethyl–7–oxo–4–thia–1–azabicyclo[3.2.0]heptane–2–carboxylic acid. It is acid–stable with good oral absorption and relatively non–toxic. It functions by inhibiting bacterial enzyme activity essential for cell biosynthesis [231, 232, 233] and exhibits a broad spectrum of action in preventing and treating various bacterial infections, including urinary [234] and respiratory infections [235], endocarditis [236], salmonellosis [237], sepsis [238], gastrointestinal infections [239], meningitis [240] and enterobacteria. The spectrum of AMP's activity is enhanced by co–administration with sulbactam, which inhibits β–lactamase activity [241]. Additionally, it demonstrates efficacy against both gram-positive and gram–negative bacteria, including *B. thuringiensis, E. coli, S. enterica, S. aureus, E. faecalis, and P. putida* [242, 243].

The anion exchange reaction was monitored using ^{1}H–NMR spectra, which confirmed the structures of modified monomers, and a summary of the results for all of them is provided in Figure 3. The efficiency of ion exchange was evaluated by analyzing

the signal assigned to the 9 protons in the trimethylammonium group and the pharmaceutical counterions (F).

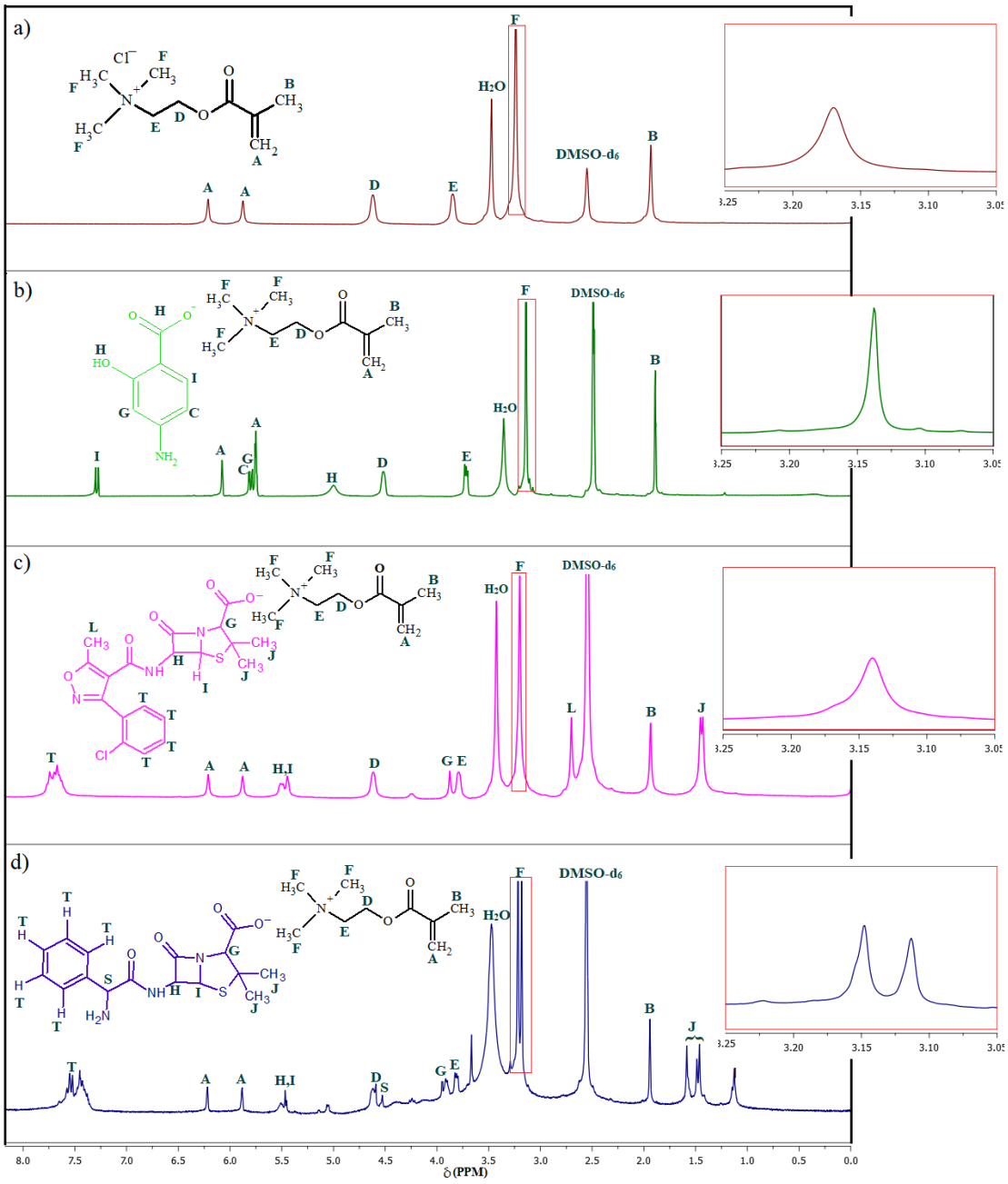

Figure 3. Summary of ^{1}H–NMR spectra of the anion exchange of monomers, TMAMA/Cl before anion exchange (a), and modified monomers including TMAMA/PAS (a), TMAMA/CLX (c), and TMAMA/AMP (d).

For TMAMA/PAS, the exchange of the chloride anion in TMAMA/Cl reached 77% efficiency after 3 hours (P.1.–Figure 2), whereas after 5 hours the exchange achieved 100% efficiency with signal F shifting from 3.18 ppm to 3.15 ppm (Figure 3b). In the case of TMAMA/CLX, the signal F shifted slightly to 3.14 ppm, signifying 100% anion exchange after 3 hours (Figure 3c). For TMAMA/AMP, signal F at 3.16 ppm split into a

doublet with maxima at 3.20 ppm and 3.12 ppm, indicating exchange efficiency of 47% after 20 hours (Figure 3d). In this case, extending the reaction time did not enhance efficiency. This could be attributed to the structure of the AMP anion, which is not beneficial for a complete exchange of chloride anion in the TMAMA.

3.2. SYNTHESIS OF LINEAR CHOLINE BASED POLYMERS BY ATRP.

Keywords: a brief overview of ATRP; functions of TMAMA and MMA; general strategy of experiments.

ATRP has proven to be a highly effective method for synthesizing well–defined linear copolymers with controlled molecular weights, narrow dispersity indices, and precisely tailored functional properties. This technique is based on a reversible redox exchange between a metal catalyst and an alkyl halide initiator, which facilitates a controlled radical polymerization process. By using ATRP, it is possible to integrate various monomers into a single polymer chain, providing excellent control over the polymer's architecture and composition [244, 245].

In this study, polymer matrices were designed using biocompatible monomers, such as biofunctionalized choline ionic liquids TMAMA and methyl methacrylate (MMA). MMA is a versatile and well-known monomer, extensively used in biomedical applications due to its combination of non-toxicity [246, 247], antimicrobial effects [248], transparency, and excellent mechanical properties [249], such as rigidity and durability. It is commonly employed in the production of bone cements [250], dental implants [251], and contact lenses [252], underscoring its importance in healthcare. However, its inherent hydrophobicity can limit its compatibility with biological systems, which explains its copolymerization with hydrophilic and functional comonomers, for example TMAMA, to enhance its biocompatibility and expand its potential for advanced medical applications [253].

The use of ATRP in the copolymerization of MMA with TMAMA provided precise control over the balance between hydrophobic and hydrophilic components within the linear copolymer matrix. This was achieved by varying the TMAMA/MMA initial ratio (e.g., f_{M1}/f_{M2} = 25/75, 50/50, 75/25) and initial ratio of monomer to initiator allowing for the fine-tuning of the copolymer's properties to meet specific functional and biocompatibility requirements of their potential as nanocarriers for DDS. The same drug content in the polymer was regulated by the content of modified TMAMA units. The linear copolymers were designed to function as either single DDS carrying PAS, AMP,

or CLX, or as dual DDS with two different pharmaceutical anions, that is PAS/AMP or CLX/AMP. In these systems, the drug anions are linked to the polymer matrix via ionic bonds. Additionally, the TMAMA/Cl without modification was polymerized to assess the impact of the pharmaceutical anion on the polymerization reaction, and then to show dependency of the physicochemical properties and drug delivery abilities on the structural characteristics of the resulting polymers. The polymers varied in several parameters, including TMAMA monomer conversion (X_{M1}) and total conversion (X) used for calculations of polymerization degree of the ionic monomer (DP_{M1}) and total degree of polymerization (DP_n), as well as the content of ionic fraction in the polymer (F_{M1}). The number-average molecular weight of the copolymers (M_n) was determined using proton nuclear magnetic resonance (^{1}H–NMR) as $M_{n,NMR}$ and size-exclusion chromatography (SEC) as $M_{n,SEC}$. Discrepancies between SEC and NMR-derived M_n values may arise due to the use of a poly(ethylene oxide) (PEO) calibration standard, which is hydrophilic but not ionic, and differs in nature from the ionic polymers. The SEC analysis was also used to determine the polymer dispersity index (Đ).

3.2.1. LINEAR POLYMER-DRUG IONIC CONJUGATES AS SINGLE DRUG DELIVERY SYSTEMS (P.1.; P.4.; P.5)

Keywords: P(TMAMA/Cl-*co*-MMA) vs. P(TMAMA/PAS-*co*-MMA) (P.1), P(TMAMA/AMP-*co*-MMA) (P.4), (TMAMA/CLX-*co*-MMA) (P.5); basic characteristics by ^{1}H-NMR and SEC; drug content by UV-Vis.

The TMAMA/Cl or pharmaceutically modified monomer TMAMA/X was copolymerized with MMA in molar ratios of 25/75, 50/50, and 75/25 at 40°C for a specified time using optimized monomer to initiator ratios (400:1 and 600:1 for TMAMA/Cl and TMAMA/PAS, 400:1 for TMAMA/AMP and TMAMA/CLX). These reactions were initiated by monofunctional ethyl 2–bromoisobutyrate (EBiB), catalyzed by a copper (I) bromide/*N*,*N*,*N*′,*N*″,*N*″- pentamethyldiethylenetriamine (CuBr/PMDETA) complex, and dissolved in a methanol/tetrahydrofuran (MeOH/THF) solvent mixture (Figure 4). They yielded the well-defined linear copolymers P(TMAMA/Cl–*co*–MMA)s (Table 1) and the well–defined polymer-drug ionic conjugates P(TMAMA/X–*co*–MMA)s varying by bioanion contents (Table 2).

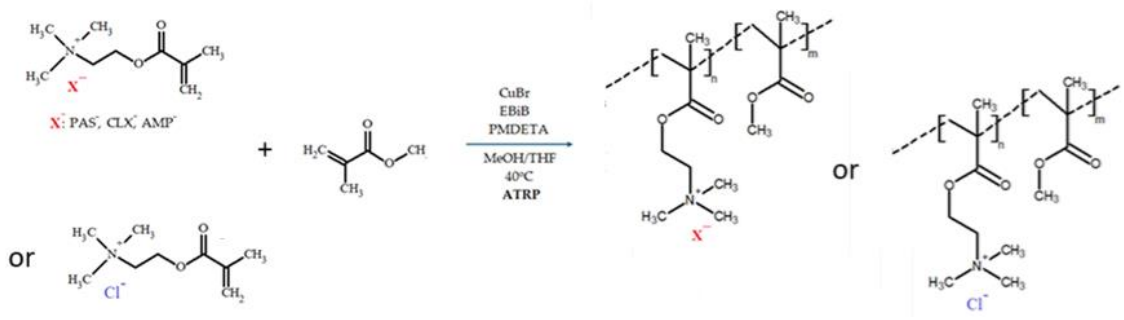

Figure 4. Reaction scheme for synthesis of linear copolymers P(TMAMA/X–*co*–MMA) or P(TMAMA/Cl–*co*–MMA) via copolymerization of TMAMA/Cl or TMAMA/X with MMA through ATRP.

Table 1. Characteristics of P(TMAMA/Cl–*co*–MMA) **L1-5** synthesized by ATRP.

			^{1}H–NMR						SEC	
No.	**f_{M1}/f_{M2} (mol %)**	**Time (h)**	**X_{M1}[a] (%)**	**X[a] (%)**	**DP_{M1}[a]**	**DP_n[a]**	**F_{M1}[a] (mol)**	**M_n[a] (g/mol)**	**M_n[b] (g/mol)**	**Đ[b]**
L1	25/75	1.5	52	51	52	203	0.26	26900	22400	1.26
L2	25/75	5	47	65	71	390	0.18	46700	47900	1.12
L3	50/50	1.7	45	45	90	179	0.50	27600	29600	1.13
L4	50/50	6.5	74	82	224	497	0.45	73800	67700	1.96
L5	75/25	2.1	44	44	132	178	0.74	31900	29900	1.14

L1-L5: M1=TMAMA/Cl; M2=MMA; conditions: $[M1+M2]_0$:$[EBiB]_0$:$[CuBr]_0$:$[PMDETA]_0$= 400:1:1:1 (except L2,L4, where $[M1+M2]_0$:$[EBiB]_0$=600:1), MeOH:TMAMA=1:1(v/w), MeOH:THF =3:1 (v/v), 40°C; X_{M1} – conversion of TMAMA/Cl. [a]in DMSO–d6, [b]in water, PEO calibration.

Table 2. Characteristics of P(TMAMA/PAS–*co*–MMA) (**I–PAS**) P(TMAMA/AMP–*co*–MMA) (**II–AMP**); P(TMAMA/CLX–*co*–MMA) (**III – CLX**) synthesized by ATRP.

			^{1}H–NMR						SEC	
No.	**f_{M1}/f_{M2} (mol%)**	**Time (h)**	**X_{M1}[a] (%)**	**X[a] (%)**	**DP_{M1}[a]**	**DP_n[a]**	**F_{M1}[a] (mol)**	**M_n[a] (g/mol)**	**M_n[b] (g/mol)**	**Đ[b]**
IA-PAS	25/75	0.66	61	66	68	272	0.25	42500	65900	1.29
IB-PAS	25/75	19	84	31	139	190	0.74	50300	51600	1.33
IC-PAS	50/50	0.91	25	32	56	133	0.42	25800	67300	1.25
ID-PAS	50/50	4	87	47	261	279	0.93	86500	212200	1.55
IE-PAS	75/25	0.73	29	37	97	162	0.60	37900	96600	1.36
IIA-AMP	25/75	27	93	33	93	131	0.71	52100	557000	1.25
IIB-AMP	50/50	20	94	77	188	308	0.61	109800	709800	1.22
IIC-AMP	75/25	21	92	91	275	363	0.76	152200	102300	1.31
IIIA-CLX	25/75	2	87	40	87	160	0.54	59900	10700	1.24
IIIB-CLX	50/50	2	90	60	179	241	0.74	115100	-	-
IIIC-CLX	75/25	2	92	75	277	299	0.93	170200	-	-

I–PAS: M1=TMAMA/PAS; M2=MMA; IIA–AMP to IIC–AMP: M1= TMAMA/AMP; III–CLX: M1=TMAMA/CLX; conditions: $[M1+M2]_0$: $[EBiB]_0$:$[CuBr]_0$:$[PMDETA]_0$= 400:1:1:1 (except IB-PAS and ID-PAS, where $[M1+M2]_0$:$[EBiB]_0$=600:1), MeOH:TMAMA=1:1(v/w), MeOH:THF =3:1 (v/v), 40°C; X_{M1} - conversion of TMAMA/PAS or TMAMA/AMP or TMAMA/CLX. [a]in DMSO–d6), [b]in water, PEO calibration, except polymers containing CLX (DMF, PEO calibration); – means not determined.

The total conversion of both monomers was calculated based on the integration of a broad signal at 0.54–1.2 ppm, corresponding to the protons in the methyl group of the polymer chain and the signals from a proton in the vinyl groups of the unreacted TMAMA and MMA monomers in the range of 5.25–6.25 ppm. Additionally, the proton signal from the vinyl group of unreacted TMAMA at 6.09 ppm, along with the proton signal from the trimethylammonium group (present in both the monomer and resulting polymer) between 2.94–3.30 ppm, was used to determine the TMAMA content. Representative spectra are presented in the original articles (P.1. –Figure 3 and 4, P.4., P.5. –Figure 3).

Linear copolymer conjugates were obtained with total monomer conversions ranging from 31 to 91%, and ionic monomer conversions between 25 to 94%. It yielded copolymers exhibited a wide range of DP_n values, but the series with AMP and CLX, indicated that equimolar or higher initial ratios of TMAMA to MMA promoted the formation of long polymer chains, exceeding 240 repeating units, even within shorter reaction times (IIB–AMP and IIC–AMP vs. IIA–AMP).

The compositions of copolymers showed the ionic fraction content in correlation with the initial content of TMAMA monomer was very well, but in some cases, it was higher than initially anticipated. The trend when $f_{M1} \sim F_{M1}$ (the PAS series: 25/25 (IA), 50/42 (IC), 75/60 (IE); the AMP series: 50/61 (IIB) and 75/76 (IIC); the Cl series: 25/26 (L1), 25/18 (L2), 50/50 (L3), 50/45 (L4), and 75/74 (L5)), indicates the copolymerization follows a statistical copolymer, suggesting similar reactivity between TMAMA and MMA. However, in cases where $f_{M1} < F_{M1}$ (the PAS series: 25/74 (IB), 50/93 (ID); the AMP series were 25/71 (IIA); the CLX series, 25/54 (IIIA), 50/74 (IIIB), and 75/93 (IIIC)), TMAMA appears to be incorporated into the polymer chain more rapidly than MMA, implying that its reactivity is higher under the given polymerization conditions. This preferential incorporation suggests a dominated gradient copolymerization process rather than a strictly statistical one. Furthermore, most of the copolymers had a narrow molecular weight distribution, as determined by SEC, with Đ values ranging from 1.12 to1.55 with exception for polymer L4 (Đ = 1.96), which had the longest chains (DP_n = 497).

The drug content (DC), representing the percentage of pharmaceutical anions incorporated into the polymer chain, evaluated by UV–Vis spectroscopy was ranged from 67–80% for CLX, 61–76% for AMP, and 24–47% for PAS (Figure 5). A simultaneous increase in DC was observed with the increase in total polymerization degree (DC / DP_n 33/133 (IC–PAS), 42/190 (IB–PAS), 47/279 (ID–PAS) as shown in Figure 5a; 61/131

(IIA–AMP), 71/308 (IIB–AMP), 76/363 (IIC–AMP) in Figure 5b; and 67/160 (IIIA–CLX), 73/241 (IIIB–CLX), 80/299 (IIIC–CLX) in Figure 5c).

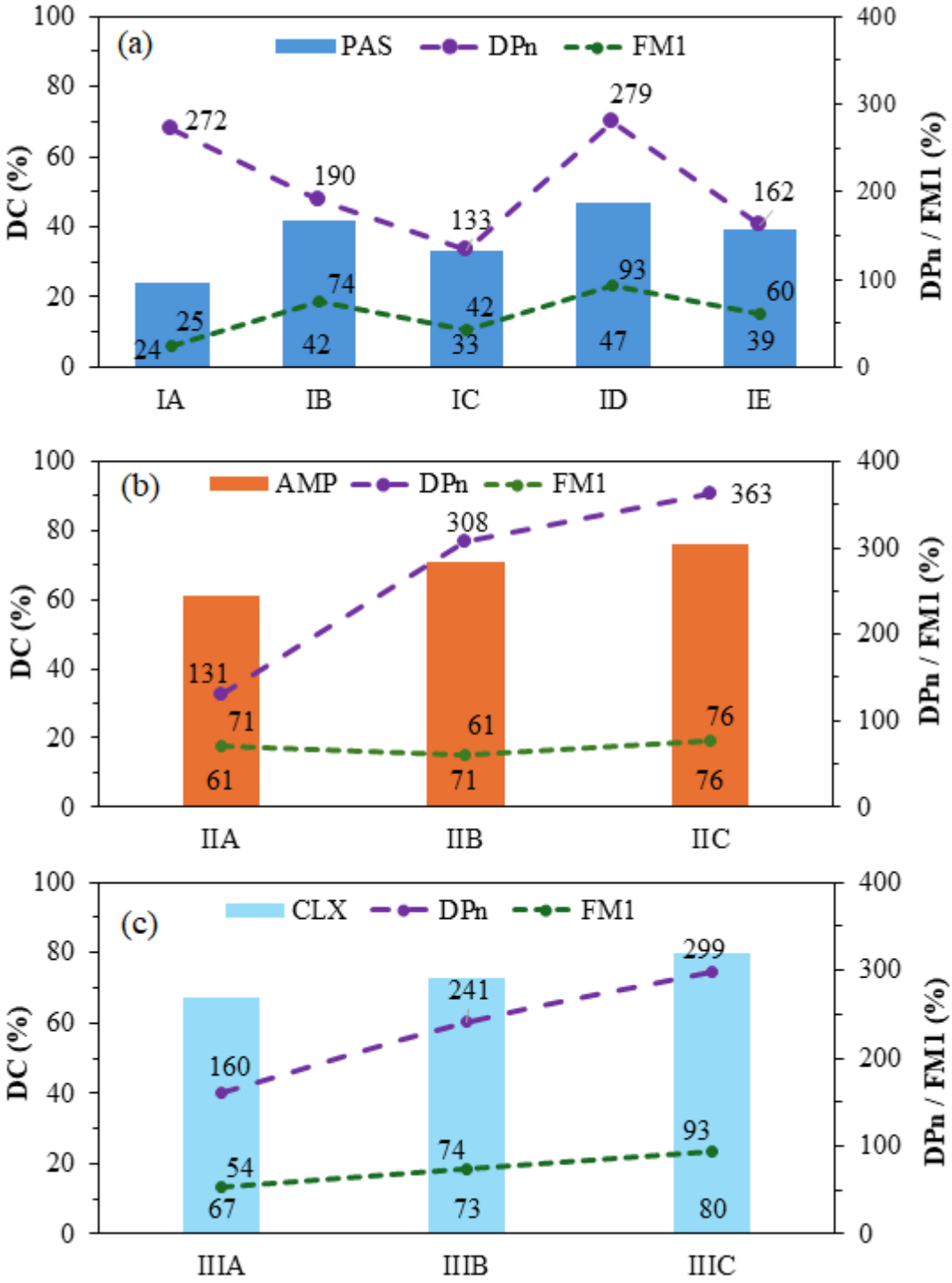

Figure 5. Summary comparing drug content (DC) for all single drug linear copolymer conjugates, containing (a) PAS, (b) AMP and (c) CLX, in relation to the ionic fraction content (F_{M1}) and polymer chain length (DP_n).

When comparing IA–PAS and IB–PAS, both with an initial TMAMA/PAS to MMA ratio of 25:75, but with differing monomer to initiator ratios for IA–PAS (400:1) and for IB–PAS (600:1), the latter achieved a higher drug content (DC = 42%). Additionally, a similar trend was observed for IC–PAS and ID–PAS, prepared with an initial TMAMA/PAS to MMA ratio of 50:50. In this case, ID–PAS (600:1) achieved a higher drug content (DC = 47%) than IC-PAS (400:1), likely due to the more diluted reaction mixture, which proved to be a more effective option for attaining higher content of TMAMA with drug counterion. The highest DC values were achieved for the longest polymer chains with the highest ionic contents (DP_n / F_{M1}(%) = 299/93 (IIIC–CLX), 363/76 (IIC–AMP), and 279/93 (ID–PAS)) making them the most advantageous systems, but in the case of PAS system drug content was double lower than for other ones (47% vs ~80%).

The reaction procedures and detailed discussions of the results are presented in the original publications (P.1, P.4, and P.5), including structural parameters such as X_{M1}, X, DP_{M1}, DP_n, F_{M1}, and M_n, which were calculated based on the ^{1}H–NMR analyses.

3.2.2. LINEAR POLYMER-DRUG IONIC CONJUGATES AS DUAL DRUG DELIVERY SYSTEMS (P.4.; P.5)

Keywords: P(TMAMA/AMP–*co*–TMAMA/PAS–*co*–MMA) (P.4), and P(TMAMA/AMP -*co*-TMAMA/CLX–*co*–MMA) (P.5); basic characteristics such as ^{1}H–NMR and SEC; drug content (DC) by UV–Vis.

The syntheses of dual drug systems were performed under the same conditions as those previously explained for the single drug copolymer conjugates. In this series, two pharmaceutically functionalized MILs, either TMAMA/AMP with TMAMA/PAS, or TMAMA/AMP with TMAMA/CLX, were copolymerized with MMA at varying initial ratios (12.5/12.5/75, 25/25/50, and 37.5/37.5/25). The resulting copolymers, P(TMAMA/AMP–*co*–TMAMA/PAS–*co*–MMA)s, named IVA–AMP+PAS to IVC and P(TMAMA/AMP–*co*–TMAMA/CLX–*co*–MMA)s, named VA–AMP+CLX to VC are shown in Figure 6 and their standard characteristics is presented in Table 3. The dual drug linear polymer conjugates were designed to co–deliver two various anion drugs simultaneously. Monomer conversion into polymer was determined by ^{1}H–NMR analysis (P.4.and P.5. –Figure 4), using analogous signals to those described for the single drug series.

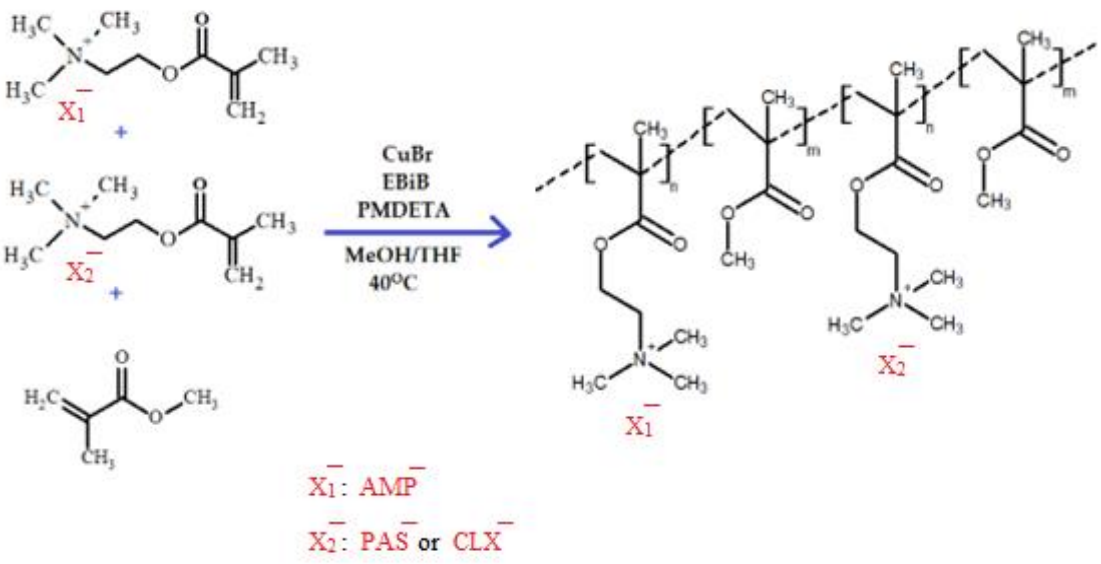

Figure 6. Reaction scheme for the synthesis of dual drug linear copolymers P(TMAMA/X1–*co*–TMAMA/X2–*co*–MMA) through copolymerization of TMAMA/X1 and TMAMA/X2 with MMA via ATRP.

Table 3. Characteristics of linear copolymers P(TMAMA/AMP–*co*–TMAMA/PAS–*co*–MMA) (IV–AMP+PAS) and P(TMAMA/AMP–*co*–TMAMA/CLX–*co*–MMA) (V–AMP+CLX) synthesized by ATRP.

			^{1}H–NMR						SEC	
No.	**f_{M1}/f_{M2} (mol %)**	**Time (h)**	**X_{M1}[a] (%)**	**X[a] (%)**	**DP_{M1}[a]**	**DP_n[a]**	**F_{M1}[a] (mol)**	**M_n[a] (g/mol)**	**M_n[b] (g/mol)**	**Đ[b]**
IVA–AMP+PAS	25/75	20	89	31	89	122	0.71	26900	173800	1.78
IVB–AMP+PAS	50/50	20	86	47	172	187	0.92	51100	95800	1.26
IVC-AMP+PAS	75/25	15	95	92	286	370	0.77	82000	161400	1.57
VA–AMP+CLX	25/75	2	91	60	91	239	0.38	55500	16200	1.58
VB–AMP+CLX	50/50	3.5	90	58	181	231	0.78	85400	–	–
VC–AMP+CLX	75/25	3	92	75	275	300	0.92	124800	–	–

Where: IVA–AMP+PAS to IVC–AMP+PAS: M1=TMAMA/AMP+TMAMA/PAS; VA–AMP+CLX to VC–AMP+CLX: M1=TMAMA/AMP+TMAMA/CLX; M2=MMA; conditions: $[M1+M2]_0$:$[EBiB]_0$:$[CuBr]_0$:$[PMDETA]_0$= 400:1:1:1; MeOH:TMAMA = 1:1 υ/ωt, MeOH:THF=3:1 υ/υ, 40°C; X_{M1} and X – conversion of both TMAMA monomers and total conversion. [a] in DMSO-d_6, [b]in water, PEO calibration (IV–AMP+PAS) and in DMF, PEO calibration (V– AMP+CLX); – means not determined.

In the dual drug polymer systems, there was an increased tendency of the polymerization degree with the initial TMAMA fraction, DP_n / f_{M1} (%): 122/25 (IVA); 187/50 (IVB); 370/75 (IVC); and 239/25 (VA); 231/50 (VB), 300/75 (VC) as shown in Table 3. Most copolymers displayed a higher ionic fraction content than predicted based on the initial ionic monomer content. The f_{M1}(%)/F_{M1}(%) were observed as follows: 25/71 (IVA), 50/92 (IVB), 75/77 (IVC), 25/38 (VA), 50/78 (VB), 75/92 (VC). Higher content of ionic fraction in copolymer suggests that under polar conditions the ionic monomer

has higher reactivity than MMA, possibly due to its preferential solubility and compatibility. However, this effect varies between the two series depending on the presence of the second drug, with PAS favoring a sharper increase at 50% TMAMA, followed by a slight decrease at 75% in IVC, which may be attributed to the saturation of solubility effects. In contrast, CLX leads to a more gradual increase across the range. This may be due to PAS being more hydrophilic than CLX, which could enhance the solubility and reactivity of the ionic monomer in the polar environment, promoting its incorporation into the polymer matrix more efficiently at intermediate concentrations. In contrast, the relatively lower hydrophilicity of CLX may lead to a more balanced interaction with the MMA, resulting in a steadier incorporation of ionic monomer across different fractions.

The controlled nature of the polymerization was confirmed by SEC results, showing low dispersity indices (Đ = 1.26). Slightly higher dispersity values (Đ ~1.6) were observed for copolymers IVC and VA, which had the longest chains (DP_n = 370 and 239, respectively) probably because of short deactivation step and fast propagation. For IVA, with the shortest chains (DP_n = 122), the dispersity increased to 1.78, likely due to the rapid incorporation of monomers before complete initiation. Additionally, SEC data for AMP+CLX systems were not obtained for copolymers with an ionic fraction above 60%, which were not soluble in DMF and water.

DC in dual drug conjugates determined by UV–Vis spectroscopy is shown in Figure 7. In IVA–IVC systems, it ranged for AMP in 71–93%, while for PAS it was significantly smaller (16–21%). In VA–VC systems, the values for AMP were similarly high, ranging from 78–87%. However, the DC for CLX in comparison to dual systems containing PAS was triple higher, ranging from 51–64%. Despite using equimolar amounts of both TMAMA monomers during polymerization, the resulting copolymers suggest that TMAMA/AMP displays higher reactivity compared to TMAMA/CLX and TMAMA/PAS, likely due to specific interactions between the two drugs. The simultaneous increase in DC was driven by the total polymerization degree and correlated with the increasing number of TMAMA units with the exception of IVC. This trend was particularly evident in VA–VC, where there was a clear relationship between the DC of both drugs, consistently showing that $DC_{CLX} < DC_{AMP}$ (VA: 51% CLX vs. 78% AMP, VB: 62% CLX vs. 83% AMP, VC: 64% CLX vs. 87% AMP). In summary, the highest DC values for CLX were achieved in VC, which had the longest polymer chain lengths and the highest ionic content (DP_n = 300 and F_{M1} = 92%), making it the most advantageous system.

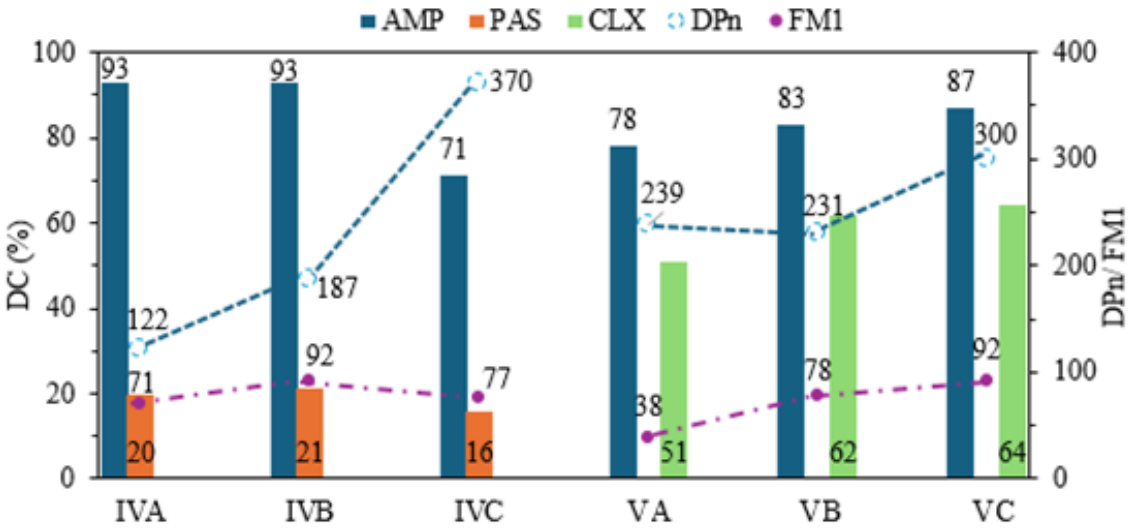

Figure 7. Summary comparing drug content (DC) for dual drug linear copolymer conjugates, in relation to the ionic fraction content (F_{M1}) and polymer chain length (DP_n).

The reaction procedures and detailed discussions of the results are reported in the original publications P.4. and P.5.

3.3. BEHAVIOR OF CHOLINE POLYMERS IN AQUEOUS SOLUTION (P.2.; P.3)

Keywords: CMC, DLS, and WCA characteristics.

The critical micelle concentration (CMC) was used to assess the ability of the selected linear copolymers (PAS based systems in comparison to chloride ones) to form self-assembling micellar structures in aqueous solution and confirming their amphiphilic properties. Interfacial tension (IFT) measurements were carried out using the pendant drop method on a goniometer for copolymer solutions and determined from the crossover point on the IFT vs. logC plot (P.2.–Figure 3), representing the concentration at which the copolymers begin to self-assemble and form micelles. The CMC results (P.2.–Table 2 and P.3.–Figure 2c) highlight the influence of ionic content on amphiphilic behavior, which in chloride based copolymers with an ionic fraction of 18–74% displayed values between 0.04 and 0.13 mg/mL (Figure 8a), whereas PAS based copolymers, with a higher ionic content (25–93%) exhibited a broader CMC range of 0.03 to 0.18 mg/mL (Figure 8b).

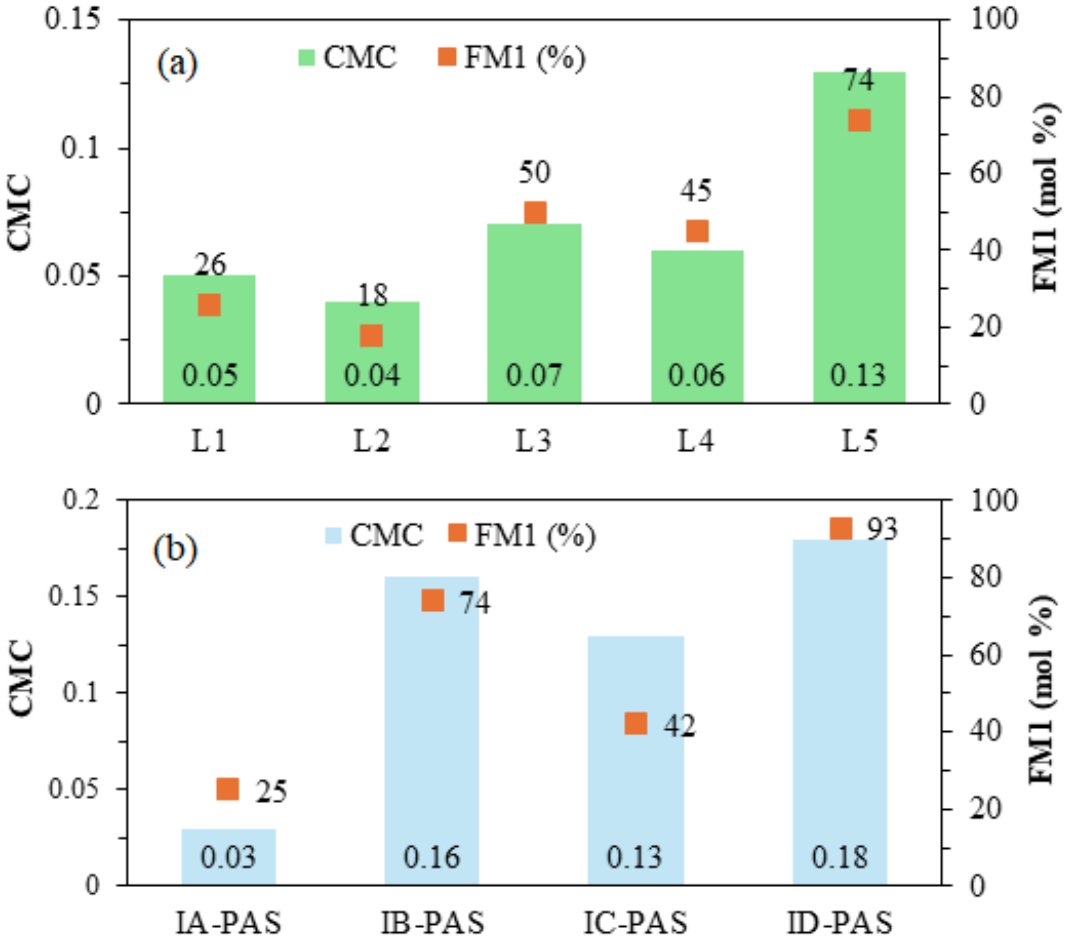

Figure 8. Dependence of CMC in relation to F_{M1} for chloride-based copolymers, L1–L5 (a) and PAS based copolymers, IA–PAS to ID–PAS (b).

For both series of linear copolymers, a clear trend was observed where the CMC value increased as the ionic fraction content increased. The type of anions in the copolymer matrix also played a significant role, influencing the interactions between copolymer chains and impacting the overall self-assembly behavior. When comparing copolymers with similar TMAMA content (~25%), chloride-based copolymers with ionic content appeared to be more hydrophilic and water-soluble than its PAS analog, which self-assembled at a lower concentration (L1 vs IA–PAS, 0.05 mg/mL vs. 0.03 mg/mL). Interestingly, for IC–PAS vs. L3, L4 and IB–PAS vs. L5 (~45% and 74% of ionic content, respectively) exhibiting relatively short chains under 200 repeating units or extremely high chain lengths (L4 ~500), the opposite CMC behavior was observed (0.13 vs. ~ 0.07 mg/mL and 0.16 vs. 0.13 mg/mL, respectively). Overall, the copolymers demonstrated low CMC values, which are advantageous for self-assembly, highlighting their potential for drug encapsulation in micellar ionic polymer systems.

The copolymer conjugates with pharmaceutical anions also demonstrated in aqueous solutions the ability to form homogeneous particles, as displayed by DLS measurements. The results for the single drug copolymer systems revealed distinct hydrodynamic diameters (Dh), ranged in 190–277 nm for AMP or CLX based ones, while IIB–AMP and IIIB–CLX displayed significantly larger diameters of 328 nm and 380 nm, respectively, as shown in Figure 9a. This size increase may be attributed to the predominant hydrophobic interactions, which encourage the formation of larger polymeric aggregates.

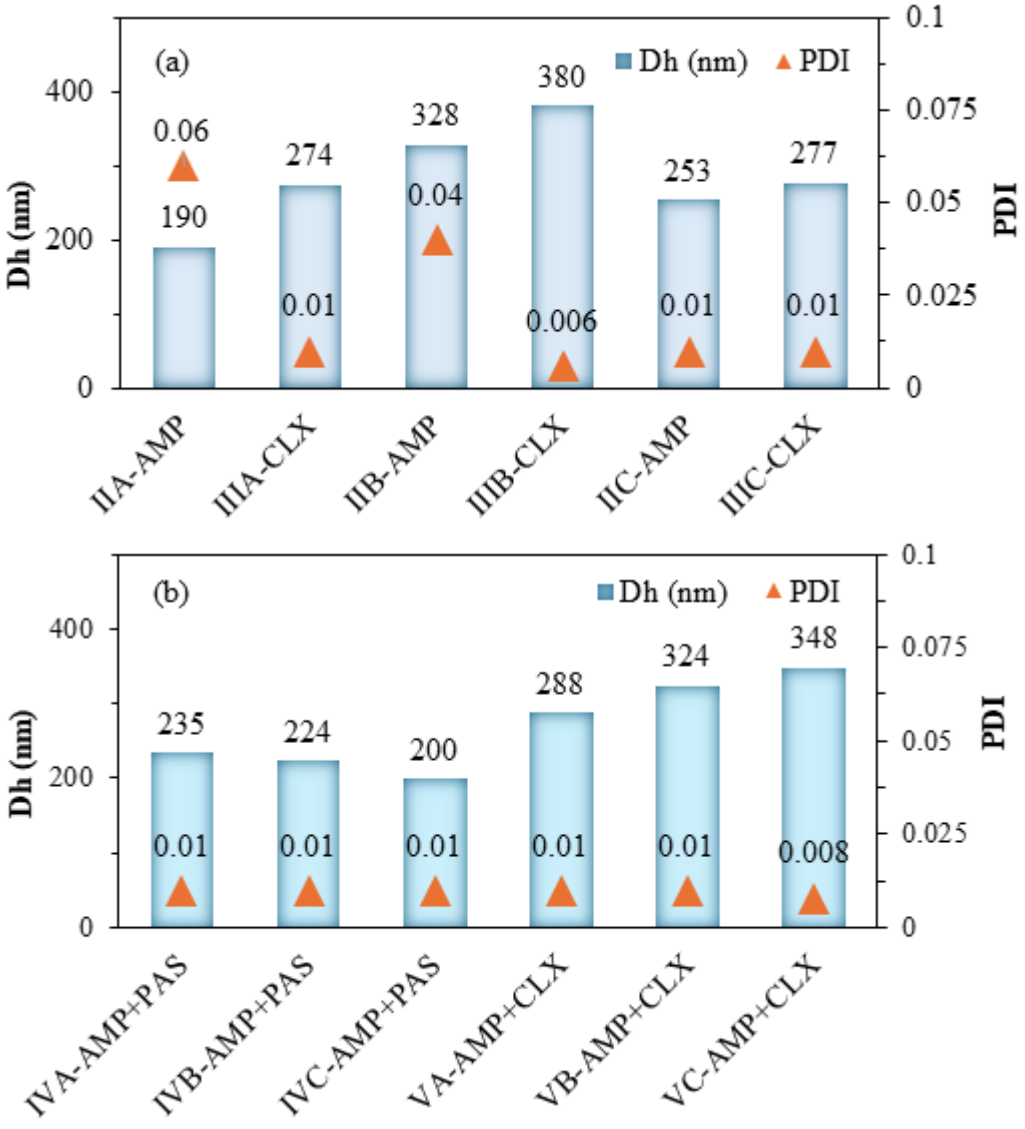

Figure 9. DLS characteristics of linear copolymer particles carrying drugs, where Dh represents the hydrodynamic diameter, and PDI stands for the polydispersity index, a) for single drug systems and b) for dual drug systems.

In the dual drug systems, the particle sizes reached 200–235 nm for the AMP/PAS series and 288–348 nm for the AMP/CLX series, as demonstrated in Figure 9b. These differences in Dh values between both series can be attributed to the different molecular structure of PAS and CLX as the accompanying to AMP. PAS, being smaller structure and likely more hydrophilic than CLX, promotes more compact particle formation and tighter packing within the polymer matrix, resulting in smaller particle sizes. The polydispersity index (PDI), which defines the level of heterogeneity of particle size distribution, indicated uniformity of particle sizes (PDI = 0.006–0.06), as demonstrated in Figure 9. The histograms showing the distribution of the formed particles exhibited one fraction (P.5.–Figure 6).

The wettability measurements were conducted using goniometry with the sessile water drop method on polymer films applied on a glass plate via spin coating to determine the water contact angle (WCA). It was measured as the parameter for evaluation of hydrophilicity or hydrophobicity degree in the polymer systems, which may be influenced by the polymer matrix structure and the nature of the incorporated drug. For chloride-based copolymers, the WCA values ranged in 53° to 35°, whereas for PAS based copolymers, the range was slightly lower from 48° to 30°, as shown in Figure 10.

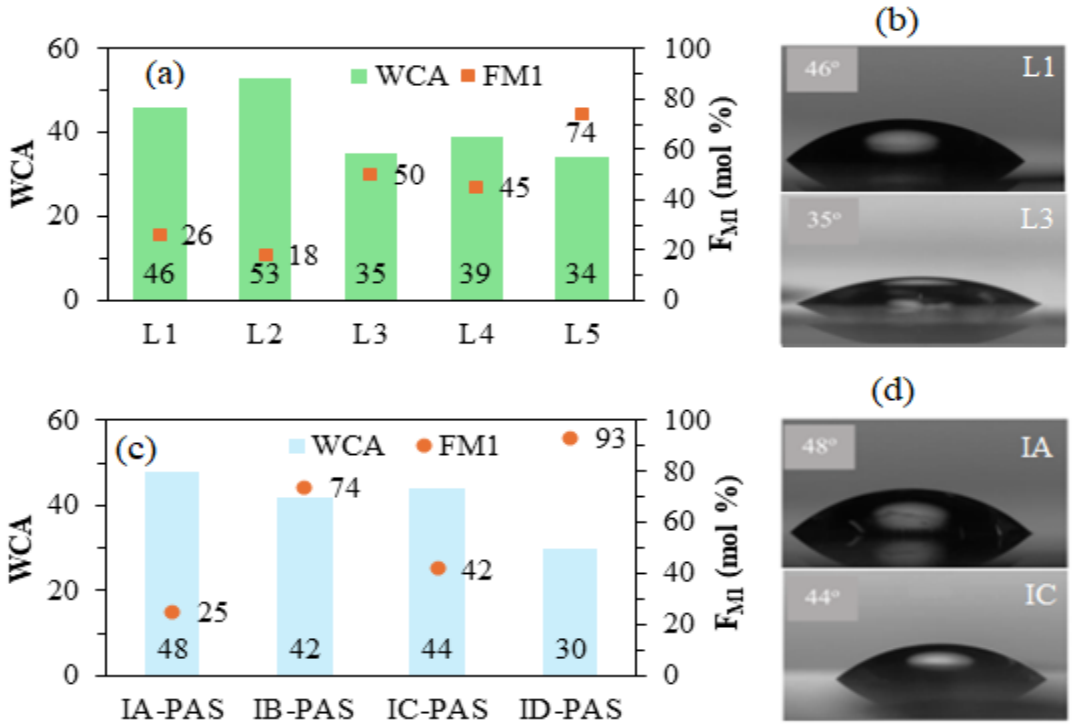

Figure 10. Dependence of WCA by goniometry using the sessile drop method on films of TMAMA/Cl–based copolymers L1–5 (a), and TMAMA/PAS based copolymer conjugates I-PAS (c) in relation to ionic content (F_{M1}), and their corresponding snapshots (b,d), The films prepared by spin-coating a 0.3 mg/mL polymer solution onto a glass plate.

The results for both series of the linear copolymers indicate that an increase in the ionic fraction content generally leads to a reduction in WCA enhancing the hydrophilicity of the copolymers, what is beneficial for solubilization of conjugated drugs. The visual changes in wettability are illustrated in photos for representative polymer samples with varying anion types and ionic fraction content.

To sum up this part of the work, the studied choline copolymers in aqueous solution displayed amphiphilic behavior to form homogeneous particles with sizes influenced by the chemical nature of the counterions and ionic fraction content, which also regulated hydrophilicity in the polymer surface.

3.4. LINEAR POLYMER CONJUGATES WITH PHARMACEUTICAL ANIONS AS MATRIXES FOR DRUG ENCAPSULATION (P.2.; P.3)

Keywords: drug encapsulation, biological functions of ISO and PAS derivatives; efficiency of encapsulation as drug loading content (DLC) by UV–Vis; DC vs DLC; WCA and DLS data for systems with encapsulated drug.

Due to the amphiphilic properties of linear copolymers and their ability to self-assemble in aqueous solutions to form stable nanoparticles, these copolymers were used as a matrix for drug encapsulation, enabling the creation of micellar drug loaded systems through dialysis method. In this study, the following model drugs, PAS in the form of acid (PASA) and sodium salt (PASNa), as well as isoniazid (ISO) (Figure 11), were selected for encapsulation. The copolymers containing chloride anions with encapsulated drug resulted in a single DDS, the same as the PAS based copolymers with encapsulated PAS to enhance efficiency of drug loading and antibacterial properties. The latter systems are especially unique because of encapsulating drug within self–assembled conjugates carrying pharmaceutical counterions, where drugs are introduced into the polymer matrix in two ways, that is in via ionic bond vs physical interactions. This approach was also applied for PAS based copolymer conjugates to encapsulate ISO yielding dual DDS.

ISO is one of the first-line antitubercular drugs used in the treatment of both active and latent for several years tuberculosis infection [254, 255]. It acts as a prodrug that is activated by the catalase–peroxidase enzyme KatG, producing radicals and adducts that block the synthesis of mycolic acids, which are crucial for the mycobacterial cell wall [256, 257] and interindividual variability in the pharmacokinetic effects [258, 259]. Additionally, ISO works synergistically with other compounds produced by KatG and

can be employed in combination therapy with another antituberculosis drug, such as the second-line PAS [260], which may prolong the effectiveness of ISO by slowing its acetylation process [261]. The biological activity of PAS was discussed in chapter 3.1.

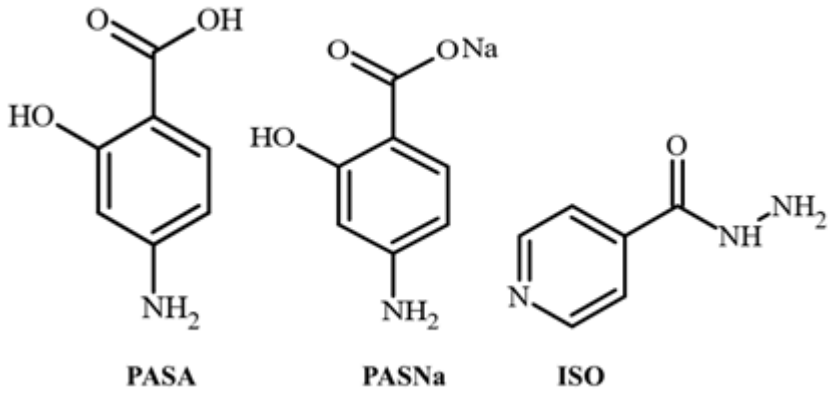

Figure 11. Chemical structure of the encapsulated drugs.

The efficiency of the encapsulation process during the self-assembly of selected linear amphiphilic copolymers was evaluated by UV–Vis analysis to determine the drug loading content (DLC) as the amount of drug incorporated into the polymer self–assemblies. DC of pharmaceutical anions in the polymer conjugates remained consistent throughout the micellization and encapsulation processes. The overall DLC varied depending on the chemical properties of the pharmaceutical substances and differences in the polymer composition, particularly the type of anions. The micellar systems of PAS–based polymers (DC = 24–47% of PAS anions), followed by additional encapsulation of PASNa (DLC = 23–52%) or PASA (DLC = 44–104%) via physical interactions (Figure 12a), proved strong potential to accommodate higher drug loads. In chloride-based copolymers (L1–L5, Figure 12b), the sodium salt of PAS may participate in ionic exchange with the chloride anions in the polymer, resulting in both physical and ionic drug binding during the encapsulation process. Comparing PAS–and chloride–based copolymers, the latter demonstrated better encapsulation efficiency, likely due to reduced steric hindrance of counterions. Furthermore, more hydrophilic PASA than PASNa was beneficial for load providing higher DLC values. The PAS– and chloride–based copolymer conjugates were also used for encapsulation of ISO with DLC values ranging in 28–43% in single DDS (L1–L4) and 30–47% in dual DDS (IA–PAS/ISO to ID–PAS/ISO), as shown in Figure 12c. The DLC decreased with increasing TMAMA content, showing an inverse relationship with the DC of PAS. These findings suggest that a higher TMAMA fraction with PAS counterions reduced the efficiency of ISO encapsulation.

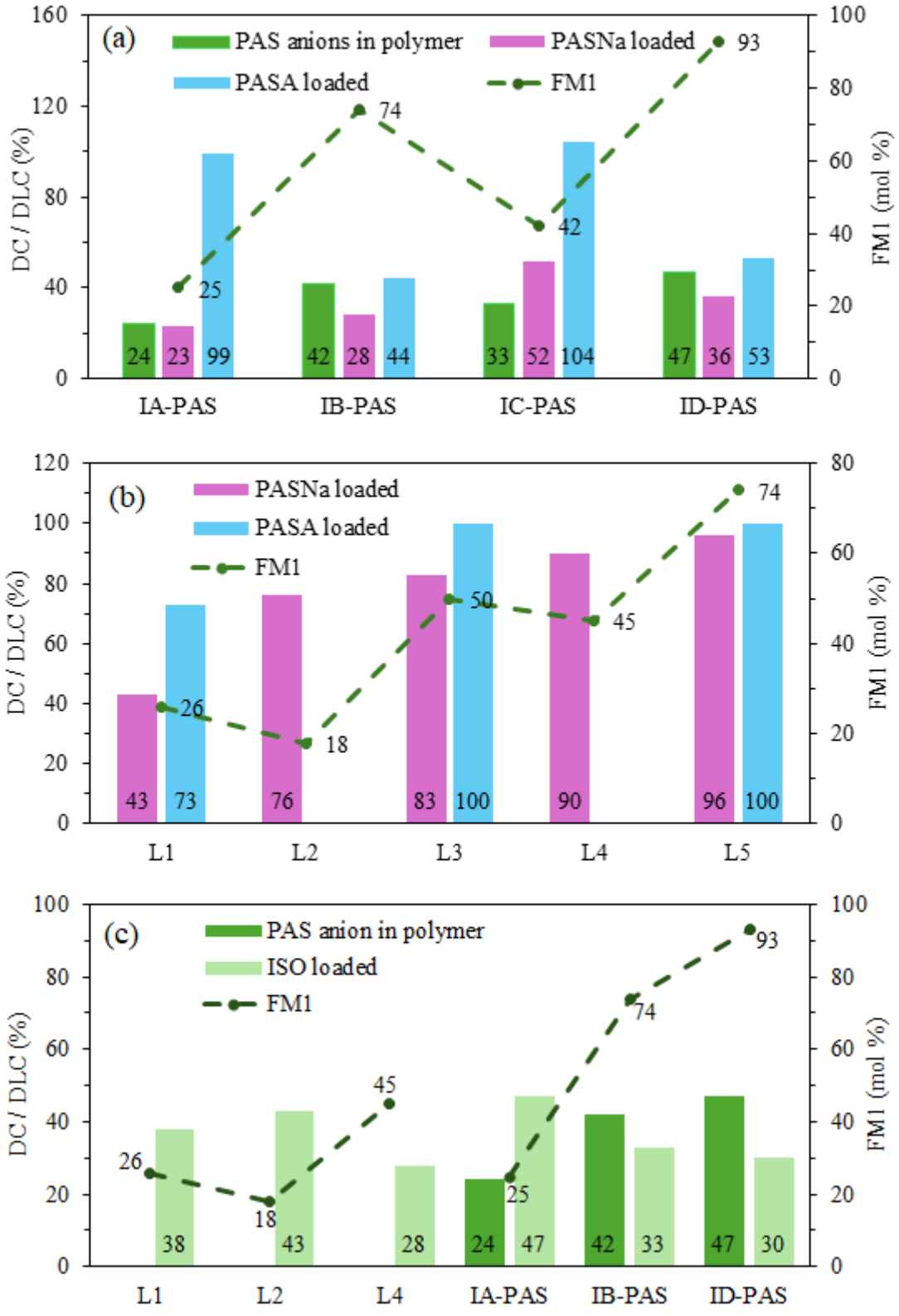

Figure 12. Relationship between drug content and the content of ionic fraction (F_{M1}) after encapsulation of PASA or PASNa (DLC) by ionic conjugates polymer–PAS (DC) (a), chloride–based copolymers (b), and ISO loaded chloride and PAS based copolymers (c).

In our studies, PASNa was found to be less hydrophilic than PASA, as indicated by higher WCA in systems with encapsulated PASNa. Additionally, systems with encapsulated PASA had higher WCA values than those without drug encapsulation (Figure 13a). This establishes the following WCA trend: non-encapsulated < PASA–encapsulated < PASNa–encapsulated, applicable to both PAS– and chloride– based systems with similar ionic content. Based on this trend, the most notable differences were observed in the ID systems, with WCA values of 30°, 42°, and 47°, respectively. These findings indicate diverse molecular arrangements of polymer chains and variations in surface characteristics. Snapshots of WCA measurements using a goniometer for various systems are shown in Figure 13b.

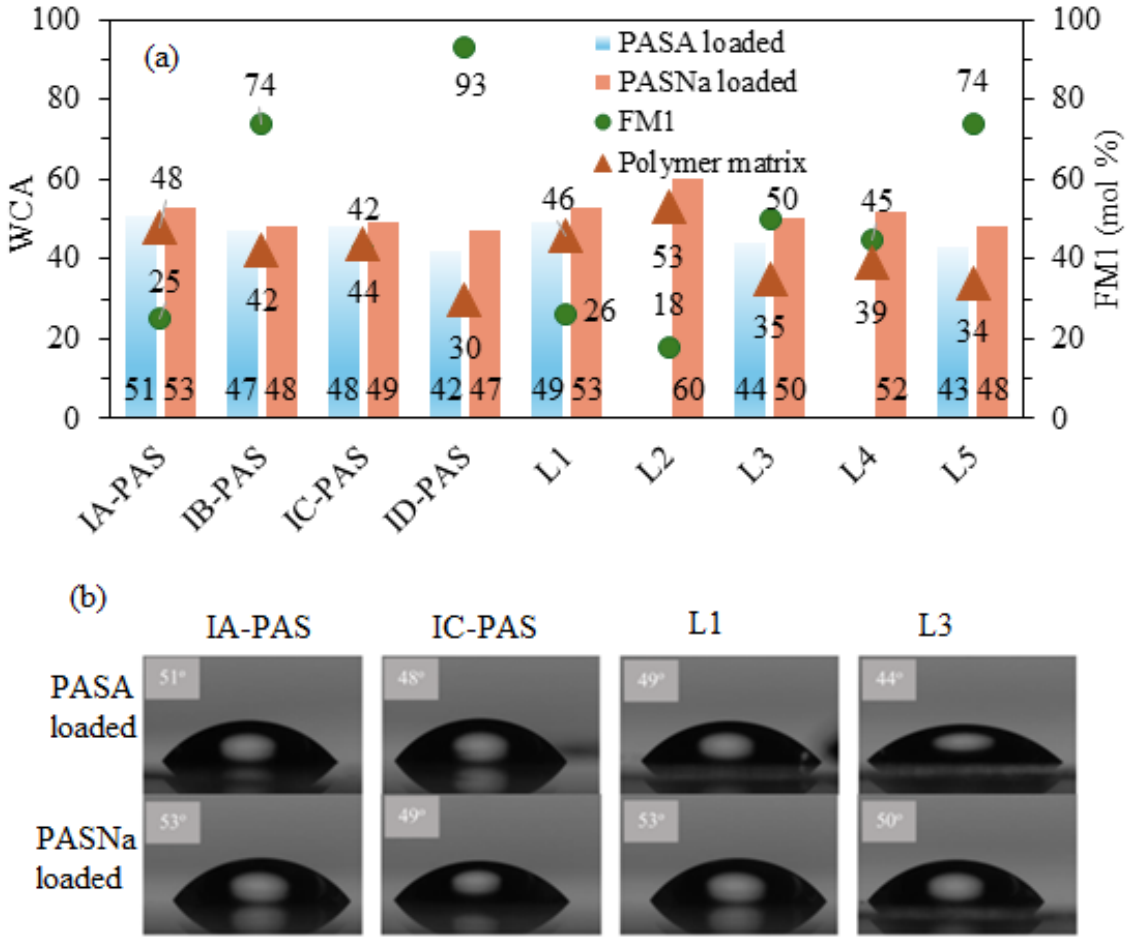

Figure 13. Dependence of WCA in relation to F_{M1} for PAS– and Cl–based copolymers encapsulated with PASA or PASNa in comparison to polymer matrix without encapsulated drug (a) and the corresponding snapshots (b).

The micellar system of PAS–based copolymer conjugates encapsulating ISO, representing dual systems containing both PAS and ISO, was analyzed by DLS to measure

the hydrodynamic diameters (Dh) of the particles in water solution as shown in Figure 14. The systems formed two prevailing fractions, and the main fraction consisted of larger superstructures ranging from 236 to 338 nm, while a fraction of the smaller particles (below 50 nm) was detected in lower amount (~ 20%). They also exhibited a significantly larger particles with sizes 1500–5000 nm due to micelle aggregation, which was attributed to the specific π–stacking interactions.

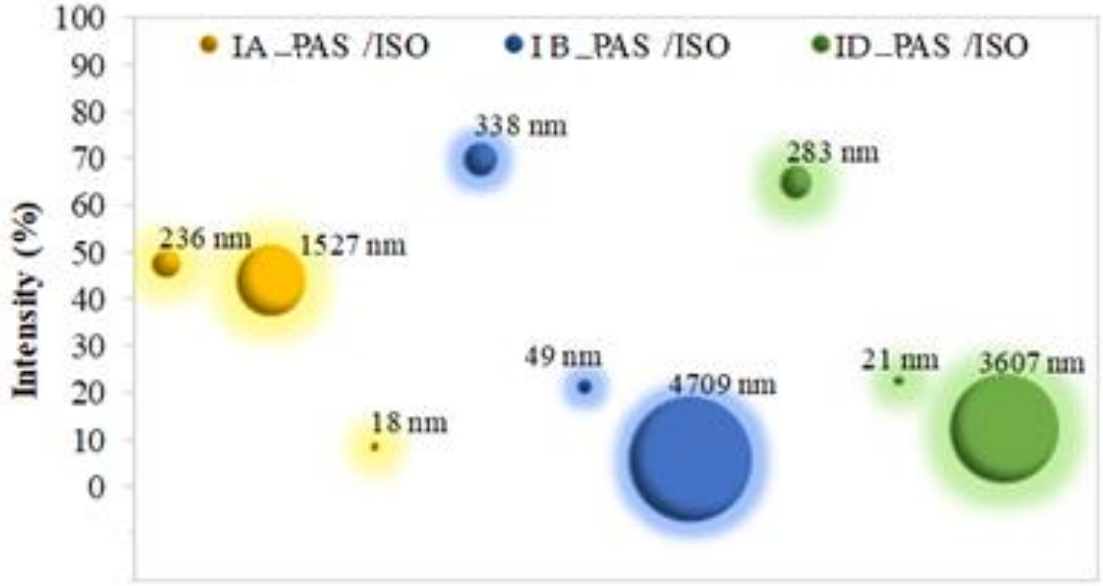

Figure 14. Particle sizes of PAS-based polymers with encapsulated ISO and distinguished fractions by DLS.

The DLC values are presented as figures in the thesis, but in the paper, they are shown in P.2.–Table 2, and P.3.–Table 1. Additionally, WCA values are presented as figures in the thesis and provided in P.2.–Table 2, and with further illustrations in P.2–Figure 6. Furthermore, a schematic illustration of the Dh of polymer nanoparticles encapsulated with ISO for fractions exceeding 30% is shown in P.3– Figure 5a.

3.5. *IN–VITRO* DRUG RELEASE STUDIES ON CHOLINE POLYMER SYSTEMS (P.1.; P.2.; P.3.; P.4.; P.5)

Keywords: mechanism release of pharmaceutical anions and encapsulated drug; drug release profiles for single and dual systems; final amount of released drug.

In vitro drug release studies were conducted using a dialysis membrane bag under physiological conditions in phosphate-buffered saline (PBS), designed to simulate human body fluids at pH 7.4 and 37°C. The drug release profiles, which display its percentage

over time, were monitored by UV–Vis spectroscopy for 72 hours. The release process was dependent on drug nature and type of its connection with polymer matrix. For pharmaceutical anions, release occurs through the ion exchange with phosphate anions in PBS, while the encapsulated drugs are released via diffusion from polymer micelles. They can offer advantages in variety of drug release rates, potentially enhancing the therapeutic effect via sequential or parallel drug co-release.

For the single PAS systems displayed notably fast release (P.1.– Figure 8), particularly for samples IB–PAS and IE–PAS (80% of released drug within the first hour). These polymers were characterized with relatively short chains and slightly dominated ionic fraction (~200 units, 60–74%), what probably generated the chain rigidity and enhanced repulsion effect, making the anions more available for release by exposing the ionic groups to the environment. Slightly different profiles were observed for systems IA–PAS and IC–PAS, where 100–80% of PAS was released after 4 hours, and in case of IA–PAS was extended to 24 hours to reach 100%. Among the series I, the IC–PAS system with the shortest chains and almost equimolar content TMAMA/MMA, demonstrated the most controlled and sustained release profile, making it particularly suitable for delivery. The ultimate ARD values are presented in Figure 15a.

Similarly, the kinetic profiles revealed a remarkably rapid release for series of the single AMP systems (P.4.– Figure 6a). Particularly for copolymer IIC–AMP featured the longest polymer chain and high AMP loading capacity in the polymer conjugates (363 units, 76%), where over 80% of AMP was released within the first hour, to achieve finally complete release (100%) after four hours. The other systems, IIA–AMP and IIB–AMP exhibited an initial burst release (~70% within four hours), followed by a more gradual release extending over 26 hours. The final values of ARD are shown in Figure 15a.

Additionally, the single CLX–based polymer conjugate systems (IIIA–CLX to IIIC–CLX), the release profiles showed an initial release of 34–41% within the first 0.5–1 hour, which increased to 58–72% by four hours and continued steadily over 74 hours with an additional 4–6% (P.5.–Figure 8a). The increase in amount of released drug (ARD), as demonstrated in Figure 15a, corresponded well with the degree of polymerization and drug content as follows: DP_n/ DC/ ARD of 160/ 67/ 58 (IIIA–CLX), 241/ 73/ 66 (IIIB–CLX), and 299/ 80/ 76 (IIIC–CLX). Combining high drug content and controlled release, copolymer IIIC–CLX emerged as the most promising candidate for extended therapeutic applications.

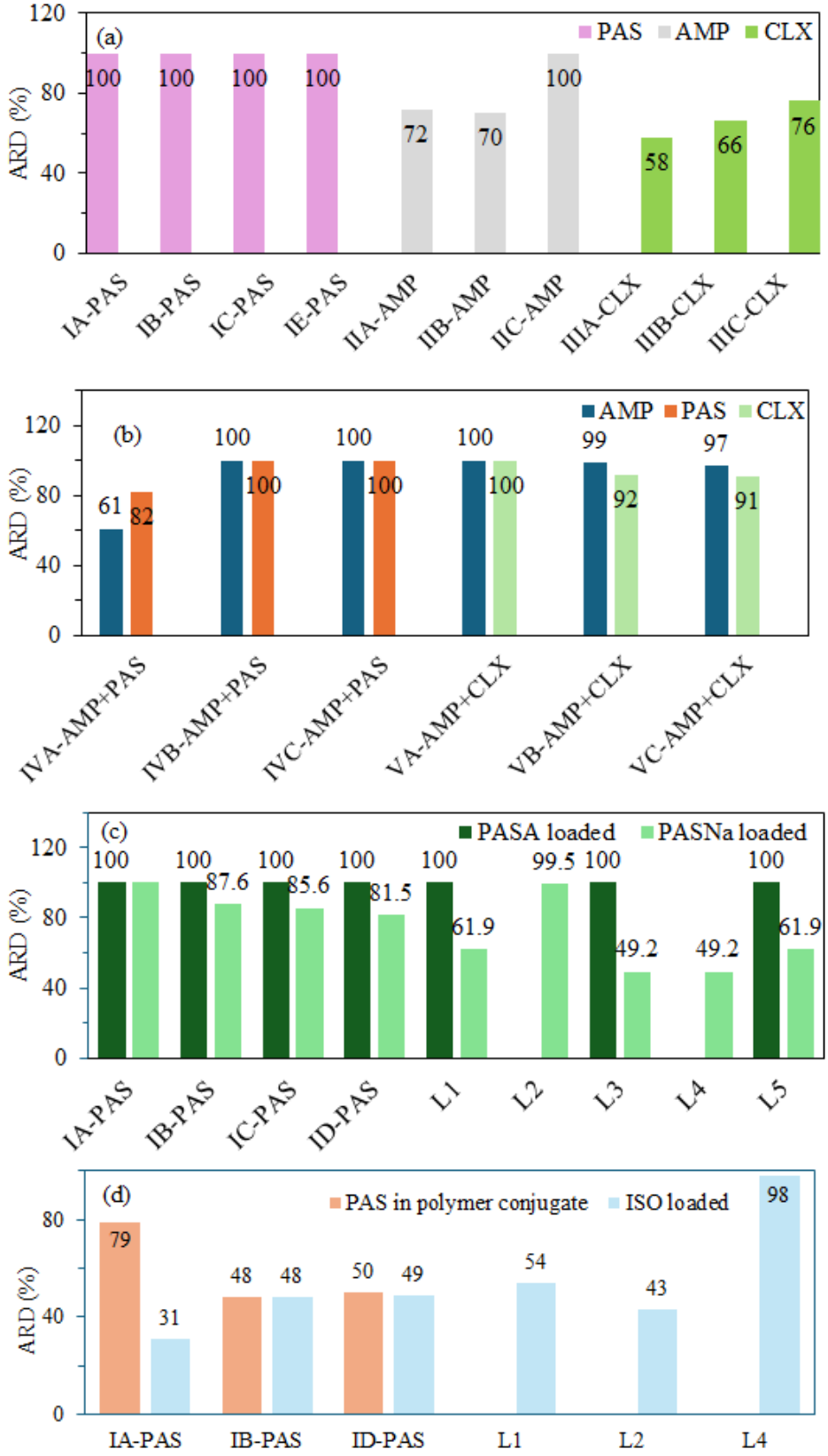

Figure 15. Amount of released drug in the conjugate systems: single (a) vs. dual (b), and in the micellar systems with the encapsulated PASNa and PASA (c), and with the encapsulated ISO (d) after 72 hours in PBS at 37°C.

In the dual AMP/PAS co–delivery systems, AMP exhibited a slower initial release (30–50% within three hours), which was in contrast to rapid initial burst of PAS (70–80% in the same period) as shown in Figure 16a. The release process continued until full release of both drugs (AMP within 70 hours and PAS after 74 hours, P.4.–Figure 6) was achieved with system IVB, which was characterized by the highest ionic content. The longest polymer chains in system IVC provided a faster and complete release of AMP (AMP within 50 hours and PAS after 74 hours). Overall, system IVB showed particularly promising potential for sustained drug delivery and co–delivery, given its drug content and release amounts, as well as effective release rate. The final values of ARD are shown in Figure 15b.

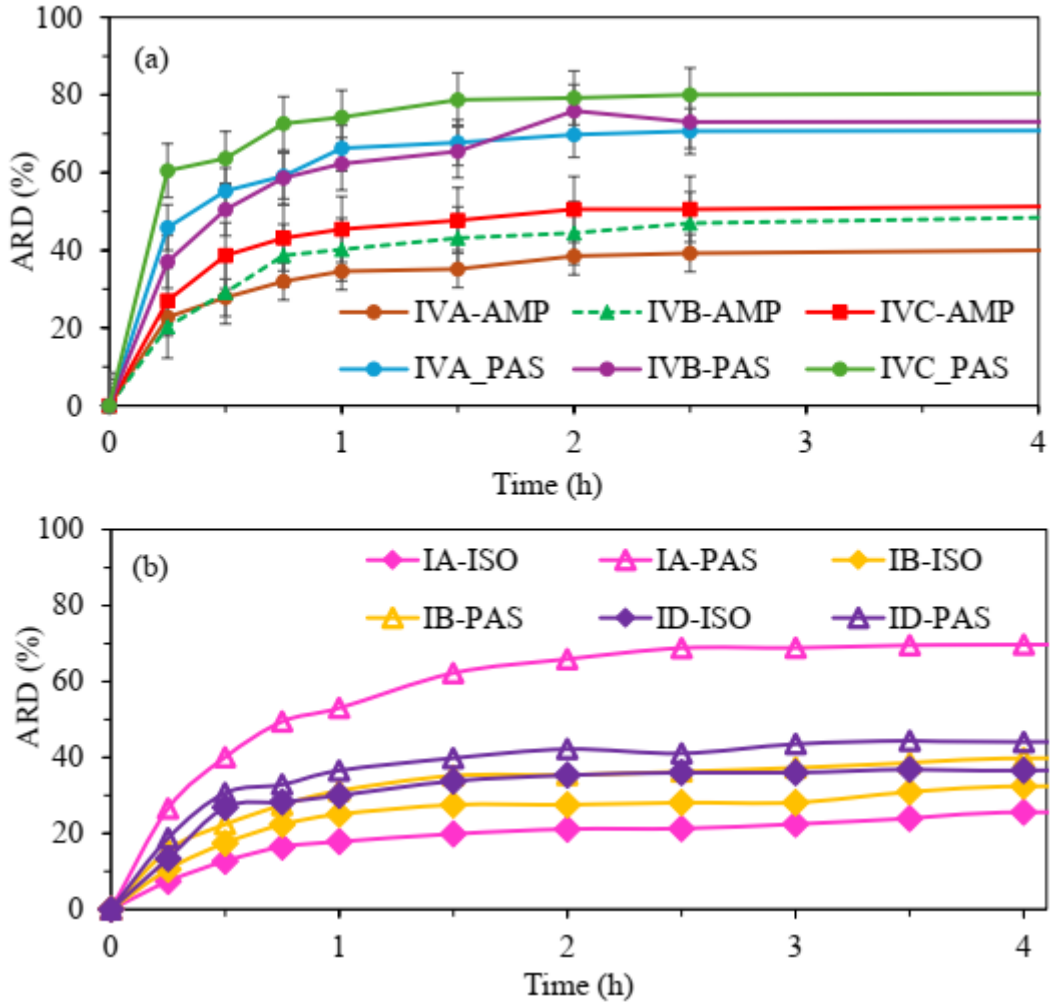

Figure 16. Representative kinetics profiles of released drugs, AMP and PAS (anion vs. anion) (a), and PAS and ISO (anion vs. encapsulated drug) (c) in dual drug systems.

In the dual AMP/CLX co-delivery systems, a significant burst release occurred within the first hour, with 64–80% of CLX (P.5.–Figure 8b) and 90–98% of AMP (P.5.–Figure 8c). Complete release of both drugs was achieved in system VA within four hours, while systems VB and VC exhibited slightly slower release rates, reaching 91–92% of CLX and 99–97% of AMP respectively. The results for dual drug series compared to single CLX series suggest that interactions between CLX and AMP enhanced the co–release of CLX in the system (Figure 15b).

In the micellar systems of PAS– and Cl–based copolymers with encapsulated PASNa, an initial burst of drug release occurred within the first hour, followed by a more gradual release over the next 12 hours. The PAS–based copolymers showed higher release amounts of PASNa with 80-100% (P.2.–Figure 8a) than Cl-based copolymers with 40–100% (P.2.–Figure 8c). For the systems encapsulating PASA, the drug release was even faster, achieving within 30 minutes full release for PAS-based copolymers (P.2.–Figure 8b) and 88–100% within 45 minutes for Cl-based copolymers (P.2.–Figure 8d), which shows minimal impact of the polymer composition on the drug release kinetics. The total ARD is demonstrated in Figure 15c.

In micellar systems of PAS– and Cl– based copolymers with encapsulated ISO, an initial burst release occurred within the first hour, as shown in (P.3.–Figure 6a and d). For the single systems, L1/ISO to L4/ISO, which are based on Cl copolymers, the release ranged from 15–29% during the first hour (P.3.–Figure 6a). In the dual PAS/ISO systems, the differences in drug co–release were lighter, but the release of PAS was approximately twice that of ISO, with 31–54% of PAS and 18–30% of ISO within first hour, as shown in Figure 16b. The final ARD values indicate that ISO was released in higher quantities from the single systems, ranging from 43–98% compared to the dual systems, which release 31–49% of the drug, as shown in Figure 15d. Additionally, in the dual systems, the ARD of ISO was similar to that of PAS (48–50%), except for IA–PAS/ISO, where a notable difference was observed, with 31% of ISO and 79% of PAS being released.

The comparison of single and dual drug systems, both in conjugate and micellar forms, highlights significant differences in release behavior. All systems typically show an initial burst followed by sustained release. Dual drug systems exhibited more complex interactions, as observed in the AMP/PAS and AMP/CLX conjugate systems. Micellar systems demonstrated rapid initial release, particularly for PAS–based copolymers. These findings confirm that the drug release rate is influenced by several factors, including

polymer structure, interactions between the bioactive anion and the polymer matrix, and drug–drug interactions.

A detailed discussion of the drug release experiments can be found in publications P.1–P.5. *In vitro* drug release profiles are presented for polymer conjugates as the single drug delivery systems (P.1.–Figure 8; P.4.–Figure 6a; and P.5.–Figure 8a), and dual drug systems (AMP and PAS in P.4.–Figures 6b and 6c; AMP and CLX in P.5.–Figures 8b and 8c) as well as for encapsulated drug systems (P.2.–Figure 8; P.3, Figure 6a).

5. SUMMARY AND CONCLUSIONS

The achievement within doctoral thesis is focused on the design of well-defined linear choline-based copolymer conjugates varying ionic contents, which were evaluated as potential carriers in single and dual DDS. Their particles in aqueous solution exhibited sizes ranging in 190–380 nm for single DDS and from 200–348 nm for dual DDS.

These polymers were synthesized via controlled radical polymerization of functionalized trimethylammonium monomers containing pharmaceutical counterions. Fo this purpose, the commercial TMAMA was modified by pharmaceutical anions with antibacterial activity, such as PAS, AMP, and CLX, through ion exchange reactions. In the single DDS, the TMAMA contents, that is 25–93 mol% in PAS series, 61–76 mol% in AMP series, and 54–93 mol% in CLX series, which was related to drug content. For the dual DDS, drugs were introduced by MILs functionalized with different anions, resulting in incorporation of TMAMA units in 38–92 mol% and 71–92 mol% for AMP/CLX series and AMP/PAS series, respectively.

As indicated in the studies, the polymer chain length, the ionic fraction content in copolymer, and the nature of pharmaceutical anion were important factors, which influenced drug content and release. The polymer matrix containing PAS (24–47%) was sufficient to achieve efficient *in vitro* release of PAS (≥80%) within 4 hours, whereas the dual drug systems of PAS/AMP (16–21%/71–93%) accomplished release in 82–100% for PAS and 61–100% for AMP within 72 hours. Similarly, the dual drug systems of AMP/CLX (78–87%/51–64%) were efficient in release of 97–100% of AMP and 91–100% of CLX within 72 hours. Their single drug systems behaved slightly different yielding release of 70–100% for AMP with the drug content of 61-76% within 26 hours and CLX with release of 58–76% and drug content of 67–80% within 72 hours. These findings demonstrate the efficacy of linear polymer conjugates in designing DDS with customizable release profiles, facilitating efficient drug delivery.

The copolymers demonstrated amphiphilic properties, forming micellar systems through self-assembly in aqueous solutions. A critical parameter for these systems was the hydrophobic fraction, which significantly influenced CMC and particle sizes. The selected series of copolymers, that is chloride series and PAS series, followed a trend where the CMC increased with an increase in the ionic fraction content (0.04–0.13 mg/mL vs 0.03–0.18 mg/mL). The anion type in water-soluble polymers impacted polymer chain interactions showing variable hydrophilicity. These findings were further confirmed by WCA measurements, which defined the degree of hydrophilicity of the surface. Additionally, the hydrodynamic diameters of polymer particles depended on the polymer chain length. Generally, the hydrophobic-hydrophilic balance, drug loading, and particle-forming capability were shown to be tunable by the copolymer structure and the characteristics of the drug, including the encapsulated drug and the combined drugs.

The amphiphilic nature of both chloride– and PAS–based copolymers enabled successful encapsulation of PAS drug, such as PASA (73–100% and 44–104%, respectively) and PASNa (43–96% and 23–52%, respectively). These findings suggest that all systems achieve high drug content suitable for PAS delivery, especially those with encapsulated PASA, where low PAS content in PAS–based polymers was efficiently completed, and chloride–based polymers at higher ionic content, yielding them the most successful systems. The majority of polymer systems achieved complete PAS release within 0.5–1 hour, but PAS–based copolymers demonstrated greater release efficiency than chloride-based systems. The same polymers were also encapsulated with ISO (28–47%) yielding both single and dual DDS, which exhibited an initial burst release within the first hour, but notably, its greater quantity was released from the single systems than the dual systems (43–98% and 31–49%, respectively). Overall, these polymer systems seem to be good candidates to effectively encapsulate and release the selected drugs.

In conclusion, the studied linear choline-based polymer conjugates with units of trimethylammonium-containing pharmaceutical anions and their micellar systems, demonstrated sufficient content of anionic drugs and strong drug encapsulation capabilities, what proved their effectiveness in developing both single and dual drug delivery systems. These systems hold significant promises for antibacterial drugs and antibiotic treatments, offering the potential for combined therapy through simultaneous drug co-delivery and enhanced therapeutic efficacy.

REFERENCES

[1] Coelho, J. F., Ferreira, P. C., Alves, P., *et al*. (2010). Drug delivery systems: Advanced technologies potentially applicable in personalized treatments. *EPMA Journal,* 1, 164–209.

[2] Zhang, Y., Chan, H. F., & Leong, K. W. (2013). Advanced materials and processing for drug delivery: the past and the future. *Adv. Drug Deliv. Rev.,* 65, 104–120.

[3] Gaurav, I., Thakur, A., Iyaswamy, A., *et al*. (2021). Factors affecting extracellular vesicles based drug delivery systems. *Molecules,* 26, 1544.

[4] Jain, K. K. (2008). Drug Delivery Systems; Springer: Berlin / Heidelberg, Germany, 251, 1–50.

[5] Lou, J., Duan, H., Qin, Q., *et al*. (2023). Advances in oral drug delivery systems: challenges and opportunities. *Pharmaceutics,* 15, 484.

[6] Majumder, J., Taratula, O., & Minko, T. (2019). Nanocarrier-based systems for targeted and site specific therapeutic delivery. *Adv. Drug Deliv. Rev.,* 144, 57–77.

[7] Visser, J. G., Van Staden, A. D. P., & Smith, C. (2019). Harnessing macrophages for controlled-release drug delivery: lessons from microbes. *Front. Pharmacol.,* 10, 22.

[8] Kingsley, J. D., Dou, H., Morehead, J., *et al*. (2006). Nanotechnology: A focus on nanoparticles as a drug delivery system. *J. N. I. P.,* 1, 340–350.

[9] Felice, B., Prabhakaran, M. P., Rodríguez, A. P., *et al*. (2014). Drug delivery vehicles on a nano-engineering perspective. *Mater. Sci. Eng. C.,* 41, 178–195.

[10] Allen, T. M., & Cullis, P. R. (2013). Liposomal drug delivery systems: From concept to clinical applications. *Adv. Drug Deliv. Rev.,* 65, 36–48.

[11] Girija, A. R. (2019). 12 - Medical applications of polymer/functionalized nanoparticle systems. *In polymer composites with functionalized nanoparticles; Pielichowski,K., Majka, T.M., Eds.; Elsevier: Amesterdam, The Netherlands,* 381–404.

[12] Demetsoz, C., & Pippa, N. (2014). Advanced drug delivery nanosystems (aDDnSs): a mini-review. *Drug. Deliv.,* 21, 250–257.

[13] Din, F. U., Aman, W., Ullah, I., *et al*. (2017). Effective use of nanocarriers as drug delivery systems for the treatment of selected tumors. *Int. J. Nanomed.,* 12, 7291–7309.

[14] Cukierman, E., & Khan, D. R. (2010). The benefits and challenges associated with the use of drug delivery systems in cancer therapy. *Biochem. Pharmacol.,* 80, 762–770.

[15] Allen, T. M., & Cullis, P. R. (2004). Drug delivery systems: Entering the mainstream. *Science,* 303,1818–1822.

[16] Ojewole, E., Mackraj, I., Naidoo, P. (2008). Exploring the use of novel drug delivery systems for antiretroviral drugs. *Eur. J. Pharm. Biopharm.,* 70, 697–710.

[17] Buddolla, A. L., & Kim, S. (2018). Recent insights into the development of nucleic acid-based nanoparticles for tumor-targeted drug delivery. *Colloids Surf. B Biointerfaces,* 172, 315–322.

[18] Duan, Q., Ma, L., Zhang, B., *et al*. (2020). Construction and application of targeted drug delivery system based on hyaluronic acid and heparin functionalised carbon dots. *Colloids Surf. B Biointerfaces,* 188, 110768.

[19] Chacko, I. A., Ghate, V. M., Dsouza, L., *et al*. (2020). Lipid vesicles: A versatile drug delivery platform for dermal and transdermal application. *Colloids Surf. B Biointerfaces,* 195, 111262.

[20] Singh, S., Pandey, V. K., Tewari, R. P., *et al*. (2011). Nanoparticle based drug delivery system: Advantages and applications. *I. J. S. T.,* 4, 177–180.

[21] Gelperina, S., Kisich, K., Iseman, M. D., *et al*. (2005). The potential advantages of nanoparticle drug delivery systems in chemotherapy of tuberculosis. *A. J. R. C. C. M.,* 172, 1487–1490.

[22] Emencheta, S. C., Onugwu, A. L., Kalu, C. F., *et al*. (2024). Bacteriophages as nanocarriers for targeted drug delivery and enhanced therapeutic effects. *Mater. Adv.,* 5, 986–1016.

[23] Farr, R., Choi, D. S., & Lee, S. W. (2014). Phage-based nanomaterials for biomedical applications. *Acta Biomater.,* 10, 1741–1750.

[24] Saraiva, C., Praça, C., Ferreira, R., *et al*. (2016). Nanoparticle-mediated brain drug delivery: Overcoming blood–brain barrier to treat neurodegenerative diseases. *J. C. R.,* 235, 34–47.

[25] Li, S., Chen, L., & Fu, Y. (2023). Nanotechnology-based ocular drug delivery systems: recent advances and future prospects. *J. Nanobiotechnology,* 21, 232.

[26] Shi, J., Votruba, A. R., Farokhzad, O. C., *et al*. (2010). Nanotechnology in drug delivery and tissue engineering: From discovery to applications. *Nano. Lett.,* 10, 3223–3230.

[27] Chen, K., Liao, S., Guo, S., *et al*. (2020). Multistimuli-responsive PEGylated polymeric bioconjugate-based nano-aggregate for cancer therapy. *Chem. Eng. J.,* 391,123543.

[28] Ofridam, F., Tarhini, M., Lebaz, N., *et al*. (2021). pH-sensitive polymers: Classification and some fine potential applications. *Polym. Adv. Technol.,* 32, 1455–1484.

[29] Ravi Kumar, M. N., & Kumar, N. (2001). Polymeric controlled drug-delivery systems: Perspective issues and opportunities. *Drug Dev. Ind. Pharm.,* 27,1–30.

[30] Bhowmik, D., Gopinath, H., Kumar, B. P., *et al*. (2012). Controlled release drug delivery systems. Pharm. Inov*.,* 1, 10.

[31] Liu, J., Huang, Y., Kumar, A., *et al*. (2014). pH-sensitive nano-systems for drug delivery in cancer therapy. *Biotechnol. Adv.,* 32, 693–710.

[32] Mura, S., Nicolas, J., & Couvreur, P. (2013). Stimuli-responsive nanocarriers for drug delivery. *Nat. Mater.,*12, 991–1003.

[33] Nguyen, D. N., Green, J. J., Chan, J. M., *et al*. (2009). Polymeric materials for gene delivery and dna vaccination. *Adv. Mater.,* 21, 847–867.

[34] Pandey, R. & Khuller, G. K. (2004). Polymer based drug delivery systems for mycobacterial infections. *Curr. Drug. Deliv.,* 1, 195–201.

[35] Kadajji, V. G., & Betageri, G. V. (2011). Water soluble polymers for pharmaceutical applications. *Polymers,* 3, 1972–2009.

[36] Vega-Vásquez, P., Mosier, N. S. & Irudayaraj, J. (2020). Nanoscale drug delivery systems: From medicine to agriculture. *Front. Bioeng. Biotechnol.,* 8, 79.

[37] Khalid, M., & El-Sawy, H. S. (2017). Polymeric nanoparticles: Promising platform for drug delivery. *Int. J. Pharm.,* 528, 675–691.

[38] Oh, J. K., Bencherif, S. A., & Matyjaszewski, K. (2009). Atom transfer radical polymerization in inverse miniemulsion: A versatile route toward preparation and functionalization of microgels/nanogels for targeted drug delivery applications. P*olymer,* 50, 4407–4423.

[39] Kamaly, N., Yameen, B., Wu, J., *et al*. (2016). Degradable controlled-release polymers and polymeric nanoparticles: mechanisms of controlling drug release. *Chem. Rev.,* 116, 2602–2663.

[40] Golan, D. E.,. Tashjian, A. H., & Armstrong, E. J. (2008). Principles of pharmacology: The pathophysiologic basis of drug therapy; Wolters Kluwer Health / *Lippincott Williams & Wilkins: Philadelphia, PA, USA,* 396, 235-258.

[41] Li, D. C., Zhong, X. K., Zeng, Z. P., *et al*. (2009). Application of targeted drug delivery system in Chinese medicine, *J. C. R.,* 138, 103–112.

[42] Rodrigues, P. R., & Vieira, R. P. (2019). Advances in atom-transfer radical polymerization for drug delivery. *Eur. Polym. J.,*115, 45–58.

[43] krys, P., & Matyjaszewski, K. (2017). Kinetics of atom transfer radical polymerization. *Eur. Polym. J.,* 89, 482–523.

[44] Matyjaszewski, K. (2012). Atom transfer radical polymerization: from mechanisms to applications. *Isr. J. Chem.,* 52, 206–220.

[45] Yazdi, M. K., Zarrintaj, P., Saeb, M. R., *et al*. (2024). Progress in ATRP-derived materials for biomedical applications. *Prog. Mater. Sci.,* 143,101248.

[46] Dashtimoghadam, E., Maw, M., Keith, A. N., *et al*. (2022). Super-soft, firm, and strong elastomers toward replication of tissue viscoelastic response. *Mater. Horiz.,* 9, 3022–3030.

[47] Dashtimoghadam, E., Fahimipour, F., Keith, A. N., *et al*. (2021). Injectable non-leaching tissue-mimetic bottlebrush elastomers as an advanced platform for reconstructive surgery. *Nat. Commun.,* 12, 3961.

[48] Yuan, L., Zhang, F., Qi, X., *et al*. (2018). Chiral polymer modified nanoparticles selectively induce autophagy of cancer cells for tumor ablation. *J. Nanobiotechnology.,* 16, 1–16.

[49] Yin, X., Hewitt, D. R., Quah, S. P., *et al*. (2018). Impact of stereochemistry on rheology and nanostructure of PLA–PEO–PLA triblocks: Stiff gels at intermediate l/d-lactide ratios. *Soft Matter,* 14, 7255–7263.

[50] Siegwart, D. J., Oh, J. K., & Matyjaszewski, K. (2012). ATRP in the design of functional materials for biomedical applications. *Prog. Polym. Sci., 37,* 18-37.

[51] Mitragotri, S., Burke, P. A., & Langer, R. (2014). Overcoming the challenges in administering biopharmaceuticals: Formulation and delivery strategies. *Nat. Rev. Drug Discov.,* 13, 655–672.

[52] Neugebauer, D., Odrobinska, J., Bielas, R., *et al*. (2016). Design of systems based on 4-armed star-shaped polyacids for indomethacin delivery. *New J. Chem.,* 40, 10002–10011.

[53] Mielanczyk, A., & Neugebauer, D. (2015). Designing drug conjugates based on sugar decorated V-shape and star polymethacrylates: Influence of composition and architecture of polymeric carrier. *Bioconjug. Chem.,* 26, 2303–2310.

[54] Bury, K., Du Prez, F., & Neugebauer, D. (2013). Self-assembling Linear and Star Shaped Poly(ϵ-caprolactone)/poly[(meth)acrylic acid] Block Copolymers as Carriers of Indomethacin and Quercetin. *Macromol. Biosci.,* 13, 1520–1530.

[55] Maksym, P., & Neugebauer, D. (2017). Self-assembling polyether-b-polymethacrylate graft copolymers loaded with indomethacin. *Int. J. Polym. Mater. Polym. Biomater.,* 66, 317–325.

[56] Maksym, P., & Neugebauer, D. (2016). Synthesis of amphiphilic semigrafted pseudo-Pluronics for self-assemblies carrying indomethacin. *RSC Adv.,* 6, 88444–88452.

[57] Bury, K., & Neugebauer, D. (2014). Novel self-assembly graft copolymers as carriers for anti-inflammatory drug delivery. *Int. J. Pharmaceut.,* 460, 150-157.

[58] Szewczyk-Łagodzinska, M., Plichta, A., Debowski, M., *et al*. (2023). Recent advances in the application of atrp in the synthesis of drug delivery systems. *Polymers,* 15, 1234.

[59] Zaborniak, I., Chmielarz, P., & Matyjaszewski, K. (2020). Synthesis of riboflavin-based macromolecules through low ppm ATRP in aqueous media. *Macromol. Chem. Phys.,* 221, 1900496.

[60] Zaborniak, I., Chmielarz, P., & Wolski, k. (2020). Riboflavin-induced metal-free ATRP of (meth) acrylates. *Eur. Polym. J.,* 140, 110055.

[61] Qin, X., Yu, C., Wei, J., *et al*. (2019). Rational design of nanocarriers for intracellular protein delivery. *Adv. Mater.,* 31, 1902791.

[62] Sung, Y. K., & Kim, S. W. (2020). Recent advances in polymeric drug delivery systems. *Biomater. Res.,* 24, 12.

[63] Li, Y., Gao, J., Zhang, C., *et al*. (2018). Stimuli-Responsive Polymeric Nanocarriers for Efficient Gene Delivery. *P. G. D. S.,* 375, 167–215.

[64] De, R., Mahata, M. K., & Kim, k. T. (2022). Structure-based varieties of polymeric nanocarriers and influences of their physicochemical properties on drug delivery profiles. *Adv. Sci.,* 9, 2105373.

[65] Boussif, O., Lezoualch, F., Zanta, M. A., *et al*. (1995). A versatile vector for gene and oligonucleotide transfer into cells in culture and in vivo: polyethylenimine. *P. N. A. S.,* 16, 7297–7301.

[66] Pant, K., Neuber, C., Zarschler, K., *et al*. (2020). Active targeting of dendritic polyglycerols for diagnostic cancer imaging. *Small,*16, 1905013.

[67] Bandyopadhyay, A., Das, T., Nandy, S., *et al*. (2023). Ligand-based active targeting strategies for cancer theranostics. *N–S Arch. Pharmacol.,* 396, 3417–3441.

[68] Narwade, M., Shaikh, A., Gajbhiye, K. R., *et al*. (2023). Advanced cancer targeting using aptamer functionalized nanocarriers for site-specific cargo delivery. *Biomater. Res.,* 27, 42.

[69] Menjoge, A. R., Kannan, R. M., & Tomalia, D. A. (2010). Dendrimer-based drug and imaging conjugates: design considerations for nanomedical applications. *Drug Discov. Today,* 15, 171–185.

[70] Krasia-Christoforou, T., & Georgiou, T. K., (2013). Polymeric theranostics: using polymerbased systems for simultaneous imaging and therapy. *J. Mater. Chem. B.,* 1, 3002–3025.

[71] Tripathi, S., Siddiqui, M. H., Kumar, A., *et al*. (2023). Nanoparticles: a promising vehicle for the delivery of therapeutic enzymes. *Int. Nano Lett.,* 13, 209–221.

[72] Zarzar, J., Shatz, W., Peer, N., *et al*. (2018). Impact of polymer geometry on the interactions of protein-PEG conjugates. *Biophys. Chem.,* 236, 22–30.

[73] Chen, D., Parayath, N., Ganesh, S., *et al*. (2019). The role of apolipoprotein-and vitronectin-enriched protein corona on lipid nanoparticles for in vivo targeted delivery and transfection of oligonucleotides in murine tumor models. *Nanoscale,* 11, 18806–18824.

[74] Zhang, X., Li, X., Zhao, Y., *et al*. (2022). Nanocarrier system: An emerging strategy for bioactive peptide delivery. *Front. nutr.,* 9, 1050647.

[75] Gohil, D., & Thirugnanasambandan, T. (2021). Nanocarriers in protein and peptide drug delivery. *Nanocarriers: DDS: An Evidence Based Approach,* Singapore: Springer Singapore, 349-365.

[76] Blin, T., Purohit, V., Leprince, J., *et al*. (2011). Bactericidal microparticles decorated by an antimicrobial peptide for the easy disinfection of sensitive aqueous solutions. *Biomacromolecules,*12, 1259–1264.

[77] Mielanczyk, A., Skonieczna, M., Mielanczyk, L., *et al*. (2016). In vitro evaluation of doxorubicin conjugates based on sugar core nonlinear polymethacrylates toward anticancer drug delivery. *Bioconjug. Chem.,* 27, 893–904.

[78] Jeon, S. I., Yang, S., Shim, M. K., *et al*. (2022). Cathepsin B-responsive prodrugs for cancer-targeted therapy: Recent advances and progress for clinical translation. *Nano Res.,* 15, 7247–7266.

[79] Yu, Y., Chen, C. K., Law, W. C., *et al*. (2013). Well defined degradable brush polymer-drug conjugates for sustained delivery of paclitaxel. *Mol. Pharm.,* 10, 867–874.

[80] Siafaka, P. I., Gündogdu, E. A., Caglar, E. S., *et al*. (2023). Polymer based Gels: Recent and Future Applications in Drug Delivery Field. *Curr. Drug Deliv.,* 20, 1288–1313.

[81] Couvreur, P., & Puisieux, F. (1993). Nano- and microparticles for the delivery of polypeptides and proteins. *Adv. Drug Deliv. Rev.,* 10, 141–162.

[82] Arora, V., Abourehab, M. A., Modi, G., *et al*. (2022). Dendrimers as prospective nanocarrier for targeted delivery against lung cancer. *Eur. Polym. J.,* 180, 111635.

[83] Huang, D., & Wu, D. (2018). Biodegradable dendrimers for drug delivery. *Mater. Sci. Eng. C.,* 90, 713–727.

[84] Yokoyama, M. (2005). Drug targeting with nano-sized carrier systems. *J. Artif. Organs,* 8, 77–84.

[85] Mackiewicz, M., Dagdelen, S., Abubakar, M. S., *et al*. (2023). Stimuli-sensitive and degradable capsules as drug carriers with decreased toxicity against healthy cells. *Polym. Degrad. Stab.,* 212, 110349.

[86] Jiang, Y., Chen, J., Deng, C., *et al*. (2014). Click hydrogels, microgels and nanogels: Emerging platforms for drug delivery and tissue engineering. *Biomaterials,* 35, 4969–4985.

[87] Oh, J. K., Drumright, R., Siegwart D. J., *et al*. (2008). The development of microgels/nanogels for drug delivery applications. *Prog. Polym. Sci.,* 33, 448–477.

[88] Miyata, K., Christie, R. J., & Kataoka, K. (2011). Polymeric micelles for nano-scale drug delivery. *React. Funct. Polym.,* 71, 227–234.

[89] Ahmad, Z., Shah, A., Siddiq, M., *et al*. (2014). Polymeric micelles as drug delivery vehicles. *RSC Adv.,* 4, 17028–17038.

[90] Hughes, K. A., Misra, B., Maghareh, M., *et al*. (2023). Use of stimulatory responsive soft nanoparticles for intracellular drug delivery. *Nano Res.,*16, 6974–6990.

[91] Hoang, N. H., Lim, C., Sim, T., *et al*. (2017). Triblock copolymers for nano-sized drug delivery systems. *J. Pharm. Investig.,* 47, 27–35.

[92] Lee, S. C., Kwon, I. K., & Park, K. (2013). Hydrogels for delivery of bioactive agents: A historical perspective. *Adv. Drug Deliv. Rev.,* 65, 17–20.

[93] Duncan, R., & Vicent, M. J. (2013). Polymer therapeutics-prospects for 21st century: The end of the beginnin. *Adv. Drug Deliv. Rev.,* 65, 60–70.

[94] Minko, T. (2005). Soluble polymer conjugates for drug delivery," *Drug Discov. Today Technol.,* 2, 15–20.

[95] Greenwald, R. B., Choe, Y. H., McGuire, J., *et al*. (2003). Effective drug delivery by PEGylated drug conjugates. *Adv. Drug Deliv. Rev.,* 55, 217–250.

[96] Jones, M. C., & Leroux, J. C. (1999). Polymeric micelles – a new generation of colloidal drug carriers. *Eur. J. Pharm. Biopharm.,* 48, 101–111.

[97] Mondon, K., Gurny, R., & Möller, M. (2008). Colloidal drug delivery systems–recent advances with polymeric micelles. *Chimia.,* 62, 832–832.

[98] Gohy, J. F. (2005). Block copolymer micelles. *Adv. Polym. Sci.,* 190, 65–136.

[99] Salem, J. K., El-Nahhal, I. M., & Salama, S. F. (2019). Determination of the critical micelle concentration by absorbance and fluorescence techniques using fluorescein probe. *Chem. Phys. Lett.,* 730, 445–450.

[100] Hamley, I. W. (2011). Self-assembly of amphiphilic peptides. *Soft Matter,* 7, 4122–4138.

[101] Li, X., Cao, C., Wei, P., *et al*. (2019). Self-Assembly of amphiphilic peptides for recognizing high furin-expressing cancer cells. *ACS Appl. Mater. Interfaces,* 11, 12327–12334.

[102] Nabiyan, A., Max, J. B., &. Schacher, F. H. (2022). Double hydrophilic copolymers – synthetic approaches, architectural variety, and current application fields. *Chem. Soc. Rev.,* 51, 995–1044.

[103] Odrobinska, J., Skonieczna, M., & Neugebauer, D. (2021). Micellar carriers of active substances based on amphiphilic peg/pdms heterograft copolymers: synthesis and biological evaluation of safe use on skin. *I. J. M. S.,* 22,1202.

[104] García, M. C. (2019). 13—Stimuli-responsive polymersomes for drug delivery applications. In Stimuli responsive polymeric nanocarriers for drug delivery applications; Woodhead Publishing: Sawston, UK, 345–392.

[105] Meng, F., Zhong, Z., & Feijen, J. (2009). Stimuli-responsive polymersomes for programmed drug delivery. *Biomacromolecules,* 10, 197-209.

[106] Maksym-Bebenek, P., & Neugebauer, D. (2015). Study on self-assembled well-defined peg graft copolymers as efficient drug-loaded nanoparticles for anti-inflammatory therapy. *Macromol. Biosci.,* 15, 1616–1624.

[107] Torchilin, V. (2001). Structure and design of polymeric surfactant-based drug delivery systems. *J. C. R.,* 73,137–172.

[108] Atanase, L. I. (2021). Micellar drug delivery systems based on natural biopolymers. P*olymers,* 13, 477.

[109] Kulthe, S. S., Choudhari, Y. M., Inamdar, N. N., *et al*. (2012). Polymeric micelles: Authoritative aspects for drug delivery. *Des. Monomers Polym.,* 15, 465–521.

[110] Yokoyama, M. (2014). Polymeric micelles as drug carriers: Their lights and shadows. *J. Drug Target.,* 22, 576–583.

[111] Haag, R. (2004). Supramolecular drug-delivery systems based on polymeric core–shell architectures. *Angew. Chem. Int. Ed.,* 43, 278–282.

[112] Figueiras, A., Domingues, C., Jarak, I., *et al*. (2022). New advances in biomedical application of polymeric micelles. *Pharmecautics,* 14, 1700.

[113] Aliabadi, H. M., & Lavasanifar, A. (2006). Polymeric micelles for drug delivery. *Expert Opin. Drug Deliv.,* 3, 139–162.

[114] Soleimani Zohr Shiri, M., Henderson, W., & Mucalo, M. R. (2019). A review of the lesser-studied microemulsion-based synthesis methodologies used for preparing nanoparticle systems of the noble metals, Os, Re, Ir and Rh. *Materials,* 12, 1896.

[115] Webber, S. E. (1998). Polymer micelles: An example of self-assembling polymers. *J. Phys. Chem. B.,* 102, 2618–2626.

[116] Hanafy, N. A., El-Kemary, M., & Leporatti, S. (2018). Micelles structure development as a strategy to improve smart cancer therapy. *Cancers,* 10, 238.

[117] Bilia, A. R., Bergonzi, M. C., Guccione, C., *et al*. (2016). Vesicles and micelles: Two versatile vectors for the delivery of natural products. *J. Drug Deliv. Sci. Technol.,* 32, 241–255.

[118] Brinkhuis, R. P., Rutjes, F. P., & van Hest, J. C. (2011). Polymeric vesicles in biomedical applications. *Polym. Chem.,* 2, 1449–1462.

[119] Zhu, Y., Yang, B., Chen, S., *et al.* (2017). Polymer vesicles: Mechanism, preparation, application, and responsive behavior. *Prog. Polym. Sci.,* 64, 1–22.

[120] Zhao, Y., Li, X., Zhao, X., *et al*. (2017). Asymmetrical polymer vesicles for drug delivery and other applications. *Front. Pharmacol.,* 8, 374.

[121] Sun, H., Wang, Y., & Song, J. (2021). Polymer vesicles for antimicrobial applications. P*olymers,* 13, 2903.

[122] Ke, X., Ng, V. W. L., Ono, R. J., *et al*. (2014). Role of non-covalent and covalent interactions in cargo loading capacity and stability of polymeric micelles. *J. C. R.,* 193, 9–26.

[123] Tang, Z., He, C., Tian, H., *et al*. (2016). Polymeric nanostructured materials for biomedical applications. *Prog. Polym. Sci.,* 60, 86–128.

[124] Ghosh, B., & Biswas, S. (2021). Polymeric micelles in cancer therapy: State of the art. *J. C. R.,* 332, 127–147.

[125] Jhaveri, A. M., & Torchilin, V. P. (2014). Multifunctional polymeric micelles for delivery of drugs and siRNA. *Front. Pharmacol.,* 5, 77.

[126] Liu, J., Lee, H., & Allen, C. (2006). Formulation of drugs in block copolymer micelles: Drug loading and release. *Curr. Pharm. Des.,* 12, 4685–4701.

[127] Fournier, E., Dufresne, M. H., Smith, D. C. *et al*. (2004). A novel one-step drug-loading procedure for water-soluble amphiphilic nanocarriers. *Pharm. Res.,* 21, 962–968.

[128] Teagarden, D. L., & Baker, D. S. (2002). Practical aspects of lyophilization using non-aqueous co-solvent systems. *Eur. J. Pharm. Sci.,* 15, 115–133.

[129] Letchford, K., Zastre, J., Liggins, R., *et al*. (2004). Synthesis and micellar characterization of short block length methoxy poly(ethylene glycol)-block-poly(caprolactone) diblock copolymers. *Colloids Surf. B Biointerfaces,* 35, 81–91.

[130] Liu, J., Zeng, F., & Allen, C. (2005). Influence of serum protein on polycarbonate-based copolymer micelles as a delivery system for a hydrophobic anti-cancer agent. *J. C. R.,* 103, 481–497.

[131] Hibino, M., Tanaka, K., Ouchi, M., *et al*. (2021). Amphiphilic random-block copolymer micelles in water: Precise and dynamic self-assembly controlled by random copolymer association. *Macromolecules,* 55, 178–189.

[132] Yokoyama, M., Satoh, A., Sakurai, Y., *et al*. (1998). Incorporation of water-insoluble anticancer drug into polymeric micelles and control of their particle size. *J. C. R.,* 55, 219–229.

[133] Minatti, E., Viville, P., Borsali, R., *et al*. (2003). Micellar morphological changes promoted by cyclization of PS-b-PI copolymer: DLS and AFM experiments. *Macromolecules,* 36, 4125–4133.

[134] Glatter, O., & Salentinig, S. (2020). Inverting structures: from micelles via emulsions to internally self-assembled water and oil continuous nanocarriers. *C. O. C. I. S.,* 49, 82–93.

[135] Rohini, N. A., Joseph, A., & Mukerji, A. (2013). Polymeric prodrugs: recent achievements and general strategies. *J. A. A.,* 15, 1–12.

[136] Khandare, J., & Minko, T. (2006). Polymer–drug conjugates: progress in polymeric prodrugs. *Prog. Polym. Sci.,* 31, 359–397.

[137] Ekladious, I., Colson, Y. L., & Grinstaff, M. W. (2019). Polymer–drug conjugate therapeutics: advances, insights and prospects. *Nat. Rev. Drug Discov.,* 18, 273–294.

[138] Kwon, G. S., & Kataoka, K. (1995). Block copolymer micelles as long-circulating drug vehicles. *Adv. Drug Deliv. Rev.,* 16, 295–309.

[139] Jatzkewitz, H. (1955). An ein kolloidales blutplasma-ersatzmittel (polyvinylpyrrolidon) gebundenes peptamin (glycyl-l-leucyl-mezcalin) als neuartige depotform für biologisch aktive primäre amine (mezcalin). *Z. naturforsch. B.,* 10, 27-31.

[140] Ringsdorf, H. (1975). Structure and properties of pharmacologically active polymers. *J. Polym. Sci. Polym. Symp.,* 51, 135–153.

[141] Junyaprasert, V. B., & Thummarati, P. (2023). Innovative design of targeted nanoparticles: polymer–drug conjugates for enhanced cancer therapy. *Pharmaceutics,* 15, 2216.

[142] Thakor, P., Bhavana, V., Sharma, R., *et al*. (2020). Polymer–drug conjugates: recent advances and future perspectives. *Drug Discov. Today,* 25, 1718–1726.

[143] Manju, S,. & Sreenivasan, K. (2011). Conjugation of curcumin onto hyaluronic acid enhances its aqueous solubility and stability. *J. Colloid. Interface. Sci.,* 359, 318–325.

[144] Huang, X., Liao, W., Xie, Z., *et al*. (2018). A pH-responsive prodrug delivery system self-assembled from acid-labile doxorubicin-conjugated amphiphilic pH-sensitive block copolymers. *Mater. Sci. Eng. C.,* 90, 27–37.

[145] Xiong, D., Zhang, X., Peng, S. *et al*. (2018). Smart pH-sensitive micelles based on redox degradable polymers as DOX/GNPs carriers for controlled drug release and CT imaging. *Colloids Surf. B Biointerfaces,* 163, 29–40.

[146] Liang, T. J., Zhou, Z. M., Cao, Y. Q., *et al*. (2016). Gemcitabine-based polymer-drug conjugate for enhanced anticancer effect in colon cancer. *Int. J. Pharm.,* 513, 564–571.

[147] Huang, D., Zhuang, Y., Shen, H., *et al*. (2018). Acetal-linked PEGylated paclitaxel prodrugs forming free-paclitaxel-loaded pH-responsive micelles with high drug loading capacity and improved drug delivery, *Mater. Sci. Eng. C.,* 82, 60–68.

[148] Issarachot, O., Suksiriworapong, J., Takano, M., *et al.* (2014). Folic acid-modified methotrexate-conjugated PEGylated poly(ε-caprolactone) nanoparticles for targeted delivery. *J. Nanoparticle Res.,* 16, 1–15.

[149] Chen, Y., Peng, F., Song, X. *et al.* (2018). Conjugation of paclitaxel to C-6 hexanediamine-modified hyaluronic acid for targeted drug delivery to enhance antitumor efficacy. *Carbohydr. Polym.,* 81, 150–158.

[150] Suksiriworapong, J., Sripha, K., Kreuter, J., *et al*. (2012). Functionalized (poly(ε-caprolactone))2-poly(ethylene glycol) nanoparticles with grafting nicotinic acid as drug carriers. *Int. J. Pharm.,* 423, 562–570.

[151] Anitha, A., Deepa, N., Chennazhi, K. P., *et al*. (2014). Combinatorial anticancer effects of curcumin and 5-fluorouracil loaded thiolated chitosan nanoparticles towards colon cancer treatment. *Biochim. Biophys. Acta (BBA)-Gen. Subj.,* 1840, 2730–2743.

[152] Larson, N., & Ghandehari, H. (2012). Polymeric conjugates for drug delivery. *Chem. Mater.,* 24, 840–53.

[153] Banerjee , S. S., Aher, N., Patil, R., *et al*. (2012). Poly(ethylene glycol)-prodrug conjugates: concept, design, and applications. *J. Drug Deliv.,* 2012, 103973.

[154] Abuchowski, A., McCoy, J. R., Palczuk, N. C., et al. (1977). Effect of covalent attachment of polyethylene glycol on immunogenicity and circulating life of bovine liver catalase. *J. Biol. Chem.,* 252, 3582–3586.

[155] Abuchowski, A., Van Es, T., Palszuk, N. C. (1977). Alteration of immunological properties of bovine serum albumin by covalent attachment of polyethylene glycol. *J. Biol. Chem.,* 252, 3578–81.

[156] Vasey, P. A., Kaye, S. B., Morrison, R., et al. (1999). Phase I clinical and pharmacokinetic study of PK1 [N-(2-hydroxypropyl)methacrylamide copolymer doxorubicin]: First member of a new class of chemotherapeutic agents-drug polymer conjugates. Cancer Research Campaign Phase I/II Committee. *Clin. Cancer Res.,* 5, 83–94.

[157] Malugin, A., Kopečková, P., & Kopeček, J. (2007). Liberation of doxorubicin from HPMA copolymer conjugate is essential for the Induction of cell cycle arrest and nuclear fragmentation in ovarian carcinoma cells. *J. C. R.,* 124, 6–10.

[158] Seymour, L. W., Ferry, D. R., Kerr, D. J., *et al*. (2009). Phase II studies of polymer-doxorubicin (PK1, FCE28068) in the treatment of breast, lung and colorectal cancer, *Int. J. Oncol.,* 34, 1629–1636.

[159] Zhang, L., Gu, F. X., Chan, J. M., *et al.* (2008). Nanoparticles in medicine: Therapeutic applications and developments. *Clin. Pharmacol. Ther.,* 83, 761-9.

[160] Alconcel, S. N., Baas, A. S., & Maynard, H. D. (2011). FDA-approved poly(ethylene glycol)–protein conjugate drugs. *Polym. Chem.,* 2, 1442–48.

[161] Karabasz, A., Bzowska, M., & Szczepanowicz, K. (2020). Biomedical applications of multifunctional polymeric nanocarriers: a review of current literature. *Int. J. Nanomed.,* 15, 8673–96.

[162] Pala, R., Anju, V. T., Dyavaiah, M., *et al*. (2020). Nanoparticle-mediated drug delivery for the treatment of cardiovascular diseases. *Int. J. Nanomed.,* 15, 3741–69.

[163] Rai, V. K., Mishra, N., Agrawal, A. K. *et al*. (2016). Novel drug delivery system: an immense hope for diabetics. *Drug Deliv.,* 23, 2371–90.

[164] Santos, L. F., Correia, I. J., Silva, A. S., *et al*. (2018). Biomaterials for drug delivery patches. *Eur. J. Pharm. Sci.,* 118, 49–66.

[165] Peer, D., Karp, J. M., Hong, S., *et al*. (2020). Nanocarriers as an emerging platform for cancer therapy. *N. H. P.,* 2, 61-91.

[166] Plechkova, N. V., & Seddon, K. R. (2007). Ionic liquids: ''designer'' solvents for green chemistry. *In: Methods Reagents Green Chem*; John Wiley and Sons, Inc., Hoboken, NJ, USA, 103–130.

[167] Mallakpour, S., & Dinari, M. (2012). Ionic liquids as green solvents: progress and prospects. in *green solvents ii: properties and applications of ionic liquids*. Springer: Berlin / Heidelberg, Germany, 1–32.

[168] Zhao, H. (2010). Methods for stabilizing and activating enzymes in ionic liquids—a review. *J. Chem. Technol. Biotechnol.,* 85, 891–907.

[169] Fukuta, T., Ikeda-Imafuku, M., & Iwao, Y. (2023). Development of edaravone ionic liquids and their application for the treatment of cerebral ischemia/reperfusion injury. *Mol. Pharmaceutics,* 20, 3115–26.

[170] Sidat, Z., Marimuthu, T., Kumar, P., *et al*. (2019). Ionic liquids as potential and synergistic permeation enhancers for transdermal drug delivery. *Pharmaceutics,* 11, 96.

[171] Adawiyah, N., Moniruzzaman, M., Hawatulaila, S., *et al*. (2016). Ionic liquids as a potential tool for drug delivery systems. *Med. Chem. Commun.,* 7, 1881-97.

[172] Wang, B., Qin, L., Mu, T., et al. (2017). Are ionic liquids chemically stable?. *Chem. Rev.,* 117, 7113-31.

[173] Marsh, K. N., Boxall, J. A., & Lichtenthaler, R. (2004). Room temperature ionic liquids and their mixtures—a review. *Fluid. Phase. Equilibria.,* 219, 93–8.

[174] Earle, M. J., & Seddon, K. R. (2000). Ionic liquids. Green solvents for the future. *Pure Appl. Chem.,* 72,1391–8.

[175] Antonietti, M., Kuang, D., Smarsly, B. (2004). Ionic liquids for the convenient synthesis of functional nanoparticles and other inorganic nanostructures. *Angew. Chem. Int. Ed.,* 43, 4988–92.

[176] Agatemor, C., Ibsen, K. N., Tanner, E. E., *et al*. (2018). Ionic liquids for addressing unmet needs in healthcare. *BioTM.,* 3, 7-25.

[177] Egorova, K. S., Gordeev, E. G., & Ananikov, V. P. (2017). Biological activity of ionic liquids and their application in pharmaceutics and medicine. *Chem. Rev.,* 117, 7132–89.

[178] Lu, J., Yan, F., & Texter, J. (2009). Advanced applications of ionic liquids in polymer science. *Prog. Polym. Sci.,* 34, 431–448.

[179] Kowsari, E. (2011). Advanced applications of ionic liquids in polymer science. Ionic liquids: Applications and perspectives. 2–28.

[180] Taha, M., Almeida, M. R., Silva, F. A., *et al*. (2015). Novel biocompatible and self-buffering ionic liquids for biopharmaceutical applications. *Chem. Eur. J.,* 21, 4781–88.

[181] Fukaya, Y., Iizuka, Y., Sekikawa, K. (2007). Bio ionic liquids: room temperature ionic liquids composed wholly of biomaterials. *Green Chem.,* 9, 1155-57.

[182] Araújo, J. M., Florindo, C., Pereiro, A. B., *et al.* (2014). Cholinium-based ionic liquids with pharmaceutically active anions. *RSC Adv.,* 4, 28126–132.

[183] García, M. T., Bautista, E., de la Fuente, A., *et al*. (2023). Cholinium-based ionic liquids as promising antimicrobial agents in pharmaceutical applications: surface activity, antibacterial activity and ecotoxicological profile. *Pharmaceutics,* 15, 1806.

[184] Messali, M., Moussa, Z., Alzahrani, A. Y., *et al*. (2013). Synthesis, characterization and the antimicrobial activity of new eco-friendly ionic liquids. *Chemosphere,* 91, 1627–34.

[185] Hu, Y., Xing, Y., Yue, H., *et al*. (2023). Ionic liquids revolutionizing biomedicine: recent advances and emerging opportunities. *Chem. Soc. Rev.,* 52, 7262–93.

[186] Li, X., Ma, N., Zhang , L. (2022). Applications of choline-based ionic liquids in drug delivery. *Int. J. Pharm.,* 612, 121366.

[187] Banerjee, A., Ibsen, K., Iwao, Y., *et al*. (2017). Transdermal protein delivery using choline and geranate (CAGE) deep eutectic solvent. *Adv. Healthc. Mater.,* 6, 1601411.

[188] Vanik, V., Bednarikova, Z., Fabriciova, G., *et al*. (2023). Modulation of insulin amyloid fibrillization in imidazolium-based ionic liquids with hofmeister series anions. *Int. J. Mol. Sci.,* 24, 9699.

[189] Ishikawa, Y., Takekiyo, T., & Yoshimu, Y. (2018). Recovery and cryopreservation of insulin amyloid using ionic liquids. *J. Mol. Liq.,* 272, 1019–24.

[190] Correia, D. M., Fernandes, L. C., Fernandes, M. M., et al. (2021). Ionic liquid-based materials for biomedical applications. *Nanomaterials,* 11, 2401.

[191] Shamshina, J. L., & Rogers, R. D. (2023). Ionic liquids: New forms of active pharmaceutical ingredients with unique, tunable properties. *Chem. Rev.,* 123, 11894–953.

[192] Shamshina, J. L., Kelley, S. P., Gurau, G., *et al*. (2015). Chemistry: Develop ionic liquid drugs. *Nature,* 528, 188–189.

[193] Pedro, S. N., Freire, C. S., Silvestre, A. J., *et al*. (2021). Ionic liquids in drug delivery. *Encyclopedia,* 1, 324-339.

[194] Jiang, L., Sun, Y., Lu, A., *et al*. (2022). Ionic liquids: Promising approach for oral drug delivery. *Pharm. Res.,* 39, 2353–65.

[195] Singh, S. K., & d Savoy, A. W. (2020). Ionic liquids synthesis and applications: An overview. *J. Mol. Liq.,* 297, 112038.

[196] Nasirpour, N., Mohammadpourfard, M., & Heris, S. Z., *et al*. (2020). Ionic liquids: Promising compounds for sustainable chemical processes and applications. *Chem. Eng. Res. Des.,* 160, 264–300.

[197] Ghandi, K. (2014). A review of ionic liquids, their limits and applications. *G. S. C.,* 4, 44–53.

[198] Gomes, J. M., Silva, S. S., & Reis, R. L. (2019). Biocompatible ionic liquids: fundamental behaviours and applications. *Chem. Soc. Rev.,* 48, 4317–35.

[199] Tao, D. J., Cheng, Z., Chen, F. F., *et al*. (2013). Synthesis and thermophysical properties of biocompatible cholinium-based amino acid ionic liquids. *J. Chem. Eng. Data.,* 58, 1542–48.

[200] Dean, P. M., Turanjanin, J., Yoshizawa-Fujita, M., *et al*. (2009). Exploring an anti-crystal engineering approach to the preparation of pharmaceutically active ionic liquids. *Cryst. Growth Des.,* 9, 1137–45.

[201] Ferraz, R., Branco, L. C., Marrucho, I. M., *et al*. (2012). Development of novel ionic liquids based on ampicillin. *MedChemComm,* 3, 494–497.

[202] Durga, G., Kalra, P., Verma, V. K., *et al*. (2021). Ionic liquids: From a solvent for polymeric reactions to the monomers for poly(ionic liquids). *J. Mol. Liq.,* 335, 116540.

[203] Maksym, P., Tarnacka, M, . Dzienia, A., et al. (2017). A facile route to well-defined imidazolium based poly (ionic liquid)s of enhanced conductivity via RAFT. *Polym. Chem.,* 8, 5433–43.

[204] Bielas, R., Mielanczyk, A., Siewniak, A., *et al*. (2016). Trimethylammonium-based polymethacrylate ionic liquids with tunable hydrophilicity and charge distribution as carriers of salicylate anions. *ACS Sustain. Chem. Eng.,* 4, 4181–91.

[205] Bielas, R., Siewniak, A., Skonieczna, M., *et al*. (2019). Choline based polymethacrylate matrix with pharmaceutical cations as co-delivery system for antibacterial and anti-inflammatory combined therapy. *J. Mol. Liq.,* 285, 114–122.

[206] Niesyto, K., & Neugebauer, D. (2021). Linear copolymers based on choline ionic liquid carrying anti-tuberculosis drugs: influence of anion type on physicochemical properties and drug release. *Int. J. Mol. Sci.,* 22, 284.

[207] Niesyto, K., & Neugebauer, D. (2020). Synthesis and characterization of ionic graft copolymers: introduction and in vitro release of antibacterial drug by anion exchange. *Polymers,* 12, 2159.

[208] Niesyto, K., Mazur, A., Neugebauer, D. (2022). Dual-drug delivery via the self-assembled conjugates of choline-functionalized graft copolymers. *Materials,* 15, 4457.

[209] Bielas, R., Łukowiec, D., & Neugebauer, D. (2017). Drug delivery via anion exchange of salicylate decorating poly(meth)acrylates based on a pharmaceutical ionic liquid. *N. J. C.,* 41, 12801–807.

[210] Bielas, R., Mielańczyk, A., Skonieczna, M., *et al*. (2019). Choline supported poly(ionic liquid) graft copolymers as novel delivery systems of anionic pharmaceuticals for anti-inflammatory and anti-coagulant therapy. *Sci. Rep.,* 9, 14410.

[211] Mazur, A., Niesyto, K., & Neugebauer, D. (2022). Pharmaceutical functionalization of monomeric ionic liquid for the preparation of ionic graft polymer conjugates. *Int. J. Mol. Sci.,* 23, 14731.

[212] Hosseinzadeh, F., Mahkam, M., & Galehassadi, M. (2012). Synthesis and characterization of ionic liquid functionalized polymers for drug delivery of an anti-inflammatory drug. *Des. Monomers. Polym.,* 15, 379–388.

[213] Gorbunova, M., Lemkina, L., & Borisova, I. (2018). New guanidine-containing polyelectrolytes as advanced antibacterial materials. *Eur. Polym. J*., 105, 426–433.

[214] Ghatak, C., Rao, V. G., Mandal, S., *et al*. (2012). An understanding of the modulation of photophysical properties of curcumin inside a micelle formed by an ionic liquid: a new possibility of tunable drug delivery system. *J. Phys. Chem. B.,* 116, 3369–79.

[215] Kurnik, I. S., D'Angelo, N. A., Mazzola, P. G., *et al*. (2021). Polymeric micelles using cholinium-based ionic liquids for the encapsulation and release of hydrophobic drug molecules. *Biomater. Sci.,* 9, 2183–96.

[216] Ali, M. K., Moshikur, R. M., Wakabayashi, R., *et al*. (2021). Biocompatible ionic liquid-mediated micelles for enhanced transdermal delivery of paclitaxel. *ACS Appl. Mater. Interfaces.,* 13, 19745–55.

[217] Lu, B., Li, Y., Wang, Z., *et al*. (2019). A dual responsive hyaluronic acid graft poly(ionic liquid) block copolymer micelle for an efficient CD44-targeted antitumor drug delivery. *New J. Chem.,* 43, 12275–82.

[218] Lu, B., Zhou, G., Xiao, F., *et al*. (2020). Stimuli-responsive poly(ionic liquid) nanoparticles for controlled drug delivery. *J. Mater. Chem. B.,* 8, 7994–8001.

[219] Mahajan, S., Sharma, R., & Mahajan, R. K. (2012). An investigation of drug binding ability of a surface active ionic liquid: micel-lization, electrochemical, and spectroscopic studies. *Langmuir,* 28, 17238–46.

[220] Moniruzzaman, M., Tahara, Y., Tamura, M., *et al*. (2020). Ionic liquid-assisted transdermal delivery of sparingly soluble drugs. *Chem. Comm.,* 46, 1452–4.

[221] Sawdon, A. J., & Peng, C. A. (2014). Polymeric micelles for acyclovir drug delivery. *Colloids. Surf. B.,* 122, 738–45.

[222] Niesyto, K., Mazur, A., & Neugebauer, D. (2024). Piperacillin/Tazobactam co-delivery by micellar ionic conjugate systems carrying pharmaceutical anions and encapsulated drug. *Pharmaceutics,* 16, 198.

[223] Donald, P. R., & Diacon, A. H. (2015). Para-aminosalicylic acid: The return of an old friend. *Lancet Infect. Dis.,* 15, 1091–99.

[224] Minato, Y., Thiede, J. M., Kordus, S. L. *et al*. (2015). Mycobacterium tuberculosis folate metabolism and the mechanistic basis for para-aminosalicylic acid susceptibility and resistance. *A. A.C.,* 59, 5097– 5106.

[225] Campregher, C., & Gasche, C. (2011). Aminosalicylates. *Best Pract. Res. Clin., Gastroenterol,* 25, 535–46.

[226] Zhang, T., Jiang, G., Wen, S. A., *et al*. (2019). Para-aminosalicylic acid increases the susceptibility to isoniazid in clinical isolates of Mycobacterium tuberculosis. *Infect. Drug Resist.,* 12, 825–29.

[227] Chang, M. J., Jin, B., Chae, J. W. (2017). Population pharmacokinetics of moxifloxacin, cycloserine, p-aminosalicylic acid and kanamycin for the treatment of multi-drug-resistant tuberculosis. *Int. J. Antimicrob. Agents.,* 49, 677–87.

[228] Knox, R., & Smith, J. T. (1963). Stability of methicillin and cloxacillin to staphylococcal penicillinase. *Br. Med. J.,* 2, 205.

[229] Legrand, T., Vodovar, D., Tournier, N., *et al*. (2016). Simultaneous determination of eight β-lactam antibiotics, amoxicillin, cefazolin, cefepime, cefotaxime, ceftazidime, cloxacillin, oxacillin, and piperacillin, in human plasma by using ultra-high-performance liquid chromatography with ultraviolet detection. *A. A. C.,* 60, 4734–42.

[230] Kohanski, M. A., Dwyer, D. J., & Collins, J. J. (2010). How antibiotics kill bacteria: from targets to networks. *Nat. Rev. Microbiol.,* 8, 423–35.

[231] Oledzka, E., Sobczak, M., Nalecz-Jawecki, G. (2014). Ampicillin-ester bonded branched polymers: characterization, cyto-, genotoxicity and controlled drug-release behaviour. *Molecules,* 19, 7543–56.

[232] Pathania, D., Verma, C., Negi, P., *et al*. (2018). Novel nanohydrogel based on itaconic acid grafted tragacanth gum for controlled release of ampicillin. *Carbohydr. Polym.,* 196, 262–71.

[233] Thottsthil, S., Puttaiahgowda, Y. M., Kanth, S. (2023). Advancement and future perspectives on ampicillin-loaded antimicrobial polymers- A review. *J. Drug. Deliv. Sci. Technol.,* 81, 104227.

[234] Shah, K. J., Cherabuddi, K., Shultz, J., *et al*. (2018). Ampicillin for the treatment of complicated urinary tract infections caused by vancomycin-resistant Enterococcus spp (VRE): a single-center university hospital experience. *Int. J. Antimicrob. Agents.,* 51, 57–61.

[235] Lode, H. (2001). Role of sultamicillin and ampicillin/sulbactam in the treatment of upper and lower bacterial respiratory tract infections. *Int. J. Antimicrob. Agents.,* 18, 199–209.

[236] Castro-Lainez, M. T., Sierra-Hoffman, M., Valladares, V. (2018). A rationale for combination ampicillin and daptomycin in renal transplant patients with enterococcal infective endocarditis. *IDCases,* 14, e00460.

[237] Eng, S. K., Pusparajah, P., Ab Mutalib, N. S., *et al*. (2015). Salmonella: a review on pathogenesis, epidemiology, and antibiotic resistance. *Front. Life. Sci.,* 8, 284–293.

[238] Gawrońska, M., Kowalik, M., & Makowski, M. (2022). Recent advances in medicinal chemistry of ampicillin: Derivatives, metal complexes, and sensing approaches. *TrAC, Trends. Anal. Chem.,* 155,116691.

[239] Kaplan, E., Ince, T., Yorulmaz, E., *et al*. (2014). Controlled delivery of ampicillin and gentamycin from cellulose hydrogels and their antibacterial efficiency. *J. Biomater. Tissue Eng.,* 4, 543–49.

[240] Pacifici, G. M. (2017). Clinical pharmacology of ampicillin in neonates and infants: effects and pharmacokinetics. *J. Ped. Perspect.,* 5, 6383–6410.

[241] Akova, M. (2008). Sulbactam-containing β-lactamase inhibitor combinations. *Clin. Microbiol. Infect*., 14, 185–188.

[242] Aumsuwan, N., Danyus, R. C., Heinhorst, S., *et al*. (2008). Attachment of ampicillin to expanded poly(tetrafluoroethylene): surface reactions leading to inhibition of microbial growth. *Biomacromolecules,* 9, 1712–18.

[243] Sabitha, M., & Rajiv, S. (2015). Preparation and characterization of ampicillin-incorporated electrospun polyurethane scaffolds for wound healing and infection control. *Polym. Eng. Sci.,* 55, 541–48.

[244] Matyjaszewski, K., & Xia, J. (2001). Atom transfer radical polymerization. *Chem. Rev.,* 101, 2921–90.

[245] Matyjaszewski, K. (2012). Atom transfer radical polymerization (ATRP): current status and future perspectives. *Macromolecules,* 45, 4015–39.

[246] Ismagilova, A., Matt, L., Jannasch, P., *et al*. (2023). Ecotoxicity of isosorbide acrylate and methacrylate monomers and corresponding polymers. *Green Chem.,* 25, 1626–34.

[247] Abed, N., & Mohammed, A. (2021). Synthesis and characterization of (methyl methacrylate/phenyl acrylamide) hydrogel for biomedical applications. *Egypt. J. Chem.,* 64, 5175–81.

[248] Juan Carlos, F. A., Rene, G. C., German, V. S., *et al*. (2020). Antimicrobial poly (methyl methacrylate) with silver nanoparticles for dentistry: a systematic review. *Appl. Sci.,* 10, 4007.

[249] Rashahmadi, S., Hasanzadeh, R., & Mosalman, S. (2017). Improving the mechanical properties of poly methyl methacrylate nanocomposites for dentistry applications reinforced with different nanoparticles. *Polym. Plast. Technol. Eng.,* 56, 1730–40.

[250] Vaishya, R., Chauhan, M., & Vaish, A. (2013). Bone cement, *J. C. O. T.,* 4, 157–163.

[251] Harpreet, K., & Archana, T. (2022). Applications of poly(methyl methacrylate) polymer in dentistry: A review. *Mater. Today.,* 50, 1619–25.

[252] Yang, M. C., Hasanah, N., & Tran-Nguyen, P. L. (2022). Effect of poly(ethylene glycol) methacrylate on the ophthalmic properties of silicone hydrogel contact lenses. *Colloids Surf. B Biointerfaces,* 217, 112713.

[253] Pituru, S. M., Greabu, M., Totan, A., *et al*. (2020). A review on the biocompatibility of PMMA-based dental materials for interim prosthetic restorations with a glimpse into their modern manufacturing techniques. *Materials,* 13, 2894.

[254] Murray, J. F., Schraufnagel, D. E., & Hopewell, P. C. (2015). Treatment of tuberculosis. a historical perspective. *AnnalsATS,* 12, 1749–59 .

[255] Soedarsono, S., Jayanti, R. P., & Mertaniasih, N. M., *et al*. (2022). Development of population pharmacokinetics model of isoniazid in Indonesian patients with tuberculosis. *I. J. I. D.,* 117, 8–14.

[256] Takayama, k., Schnoes, H. K., Armstrong, E. L., *et al*. (1975). Site of inhibitory action of isoniazid in the synthesis of mycolic acids in Mycobacterium tuberculosis. *J. L. R.,* 16, 308–17.

[257] Jindani, A., Aber, V. R., Edwards, E. A., *et al*. (1980). The early bactericidal activity of drugs in patients with pulmonary tuberculosis. *Am. Rev. Respir. Dis.,*121, 939–49.

[258] McIlleron, H., Wash, P., Burger, A., *et al*. (2006). Determinants of rifampin, isoniazid, pyrazinamide, and ethambutol pharmacokinetics in a cohort of tuberculosis patients. *A. A. C.,* 50, 1170–7.

[259] Kinzig-Schippers, M., Tomalik-Scharte, D., Jetter, A., *et al*. (2005). Should we use n-acetyltransferase type 2 genotyping to personalize isoniazid doses? *A. A. C.,* 49, 1733–8.

[260] Zhang, T., Jiang, G., Wen, S. A., *et al*. (2019). Para-aminosalicylic acid increases the susceptibility to isoniazid in clinical isolates of Mycobacterium tuberculosis. *Infect. Drug Resist.,* 12, 825–9.

[261] Jennne, J. W. (1965). Partial purification and properties of the isoniazid transacetylase in human liver. Its relationship to the acetylation of *p*-aminosalicylic acid. *J. Clin. Invest.,* 44, 1992–2002.

LIST OF FIGURES AND TABLES

Figure 6. Reaction scheme for the synthesis of dual drug linear copolymers P(TMAMA/X1–*co*–TMAMA/X2–*co*–MMA) through copolymerization of TMAMA/X1 and TMAMA/X2 with MMA via ATRP.

Figure 7. Summary comparing drug content (DC) for dual drug linear copolymer conjugates, in relation to the ionic fraction content (F_{M1}) and polymer chain length (DP_n).

Figure 8. Dependence of CMC in relation to F_{M1} for chloride-based copolymers, L1–L5 (a) and PAS based copolymers, IA–PAS to ID-PAS (b).

Figure 9. DLS characteristics of linear copolymer particles carrying drugs, where Dh represents the hydrodynamic diameter, and PDI stands for the polydispersity index, a) for single drug systems and b) for dual drug systems.

Figure 10. Dependence of WCA by goniometry using the sessile drop method on films of TMAMA/Cl–based copolymers L1–5 (a) and their corresponding snapshots (b), as well as TMAMA/PAS based copolymer conjugates IA–PAS to D (c) and their snapshots (d), in relation to ionic content (F_{M1}). The films were prepared by spin-coating a 0.3 mg/mL polymer solution onto a glass plate.

Figure 11. Chemical structure of the encapsulated drugs.

Figure 12. Relationship between drug content and the content of ionic fraction (F_{M1}) after encapsulation of PASA or PASNa (DLC) by ionic conjugates polymer–PAS (DC) (a), chloride–based copolymers (b), and ISO loaded chloride and PAS based copolymers (c).

Figure 13. Dependence of WCA in relation to F_{M1} for PAS- and Cl-based copolymers encapsulated with PASA or PASNa in comparison to polymer matrix without encapsulated drug (a) and their corresponding snapshots (b).

Figure 14. Particle sizes of PAS-based polymers with encapsulated ISO and distinguished fractions by DLS.

Figure 15. Amount of released drug in the conjugate systems: single (a) vs. dual (b), and in the micellar systems with the encapsulated PASNa and PASA (c) and with the encapsulated ISO (d) after 72 hours in PBS at 37ºC.

Figure 16. Representative kinetics profiles of released drugs, AMP and PAS (anion vs. anion) (a), and PAS and ISO (anion vs. encapsulated drug) (c) in dual drug systems.

Table 1. Characteristics of P(TMAMA/Cl–*co*–MMA) L1-5 synthesized by ATRP.

Table 2. Characteristics of P(TMAMA/PAS–*co*–MMA) (I–PAS) P(TMAMA/AMP–*co*–MMA) (II–AMP); P(TMAMA/CLX–*co*–MMA) (III – CLX) synthesized by ATRP.

Table 3. Characteristics of linear copolymers P(TMAMA/AMP–*co*–TMAMA/PAS–*co*–MMA) (IV-AMP+PAS) and P(TMAMA/AMP–*co*–TMAMA/CLX–*co*–MMA) (V-AMP+CLX) synthesized by ATRP.

LIST OF SCIENTIFIC ACHIEVEMENTS

Publications derived from PhD thesis

1. Keihankhadiv, S., & Neugebauer, D**.** Synthesis and characterization of linear copolymers based on pharmaceutically functionalized monomeric choline ionic liquid for delivery of *p*-aminosalicylate. *Pharmaceutics*. **2023**, *15*(3), p.860**.** (IF_{2022}=5.4; MEiN= 140pkt)

2. Keihankhadiv, S., & Neugebauer, D. Self-assembling polymers with p-aminosalicylate anions supported by encapsulation of p-aminosalicylate for the improvement of drug content and release efficiency. *Pharmaceuticals*, **2023**, *16*(10), p.1502. (IF_{2022}= 4.67; MEiN= 140 pkt)

3. Niesyto, K., **Keihankhadiv, S**., Mazur, A., Mielańczyk, A. and Neugebauer, D. Ionic liquid-based polymer matrices for single and dual drug delivery: impact of structural topology on characteristics and in vitro delivery efficiency. *International Journal of Molecular Sciences*, **2024**, *25*(2), p.1292. (IF_{2022}=5.6; MEiN=140 pkt)

4. Keihankhadiv, S., & Neugebauer, D. Simple strategy of the use of pharmaceutically functionalized ionic liquids in a new generation of polymer nanocarriers for the combined delivery of ionic *p*-aminosalicylate and ampicillin. *International Journal of Pharmaceutics*, **2024**, *662*, p.124483. (IF_{2022}=5.8; MEiN=100 pkt, CS-hp2023=92).

5. Keihankhadiv, S., & Neugebauer, D**.** Polymerizable cholinium-based antibiotics for polymer carriers: systems with combined load of cloxacillin and ampicillin. *Molecules*, **2024**, *29*(24), p.5973. (IF_{2023}=4.2; MEiN=140 pkt, CS-hp2023=83).

Total IF: 25.67

Patent applications

Keywords: I have three patent applications from my PhD thesis

Z.1. Method of obtaining ion conjugates for co-delivery of drugs with antibacterial activity and their use
Keihankhadiv, S., Niesyto, K., Mazur, A., Neugebauer, D.
National patent application P.446976 dated 04.12.2023

Z.2. Method of obtaining ion conjugates for the delivery of drugs with antibacterial activity and their use
Keihankhadiv, S., Niesyto, K., Mazur, A., Neugebauer, D.
National patent application P.446981 dated 04.12.2023

Z.3. Method of obtaining micellar ion conjugates based on linear polymers for co-supply of antituberculosis drugs and their application
Keihankhadiv, S., Niesyto, K., Neugebauer, D.
National patent application P.446972 of 04.12.2023

Conference presentation

2022

Keihankhadiv, S., & Neugebauer, D. Studies on the well-defined choline ionic liquid linear copolymers carrying p-aminosalicylate: synthesis, physicochemical characterization and in vitro drug release. XXVI Gliwice Scientific Meetings; Gliwice, 18-19/11/2022, **p.**167

2023

Keihankhadiv, S., & Neugebauer, D. Drug delivery through encapsulation of self-assembled linear copolymer conjugates. Inter Nano Poland; Katowice, 11-12/10/2023, **p.**98

Keihankhadiv, S., & Neugebauer, D. Micellar drug-loaded systems via encapsulation of p-aminosalicylate in amphiphilic linear copolymer matrixes. XXVI Gliwice Scientific Meetings. Gliwice, 16-17/11/2023, **p.**126

2024

Keihankhadiv, S., & Neugebauer, D. self-assembled micelles based on amphiphilic linear copolymer conjugates for delivery of antituberculosis drugs. XXIII Scientific Conference – Controlled Polymerization. Łódź, 03/06/2024. **p**.8

Keihankhadiv, S., & Neugebauer, D. ATRP-synthesized linear copolymer conjugates from pharmaceutically functionalized choline ionic liquid monomers for ampicillin delivery. The 1st International Online Conference on Functional Biomaterials-MDPI, Online, sciforum-089892, 10-12/07/2024. **p.**103.

Keihankhadiv, S., & Neugebauer, D. Linear poly(ionic liquid)-cloxacillin conjugates: a novel drug delivery system, Inter Nano Poland, Katowice, 16-17/10/2024. **p.48.**

Keihankhadiv, S., & Neugebauer, D. Dual drug delivery systems based on linear poly(ionic liquid) conjugates carrying *p*-aminosalicylate and ampicillin. Young science beyond borders, Online, 24-25/10/2024, p. 88-89.

Keihankhadiv, S., & Neugebauer, D. Poly(Ionic Liquid) nanoparticles synthesized via ATRP for drug delivery application. PhD-Nexus 2024, Wisła, 25/10/2024.

Keihankhadiv, S., & Neugebauer, D. Polymer nanostructures synthesized by atom transfer radical polymerization for drug delivery. XXVIII Gliwice Scientific Meetings, Gliwice, 21-22/11/ 2024, p. 198.

Statutory projects of the Silesian University of Technology

1. Design and characterization of linear copolymer containing pharmaceutically functionalized monomeric choline ionic liquid for delivery of naproxen or other pharmaceutical anion
BKM- 546/RCH4/2023 (04/040/BKM23/0260)

2. ATRP-synthesized linear copolymer based on ionic liquid functionalized with cloxacillin and ampicillin for single- and dual-drug delivery systems
BKM-539/RCH4/2024 (04/040/BKM24/0288)

Workshops

"Progress in controlled polymerization" Prof. Krzysztof Matyjaszewski
National Scientific Workshops organized by the Centre of Molecular and Macromolecular Studies of the Polish Academy of Sciences in Łódź, Poland. 2023

Scholarships and awards

1. Fully funded PhD scholarship from the Silesian University of Technology (2021-2025).
2. Awarded an Erasmus + scholarship for a one-month traineeship in 2025.

Traineeship

Title:

Evaluation of the morphology and crystallization of multi-component biobased polymeric systems (blends and random copolymers)

Description:

This traineeship, part of the Erasmus+ program, was from February 1st to March 2nd, 2025, within Prof. Alejandro J. Muller's research group. Prof. Muller is an IKERBASQUE Research Professor affiliated with POLYMAT and the University of the Basque Country (UPV/EHU). This project conducted at the Department of Polymers and Advanced Materials: Physics, Chemistry, and Technology, within the Faculty of Chemistry at UPV/EHU, located at Paseo Manuel de Lardizabal 3, 20018, Donostia-San Sebastián, Spain.

Evaluation of the trainee:

(Written by Prof. Alejandro J. Muller)
In this short internship, the trainee showed interest in learning different characterization techniques and carried out many experiments given the short time. The objectives of the internship were, therefore, successfully carried out. In my opinion, the trainee deserves full recognition (10/10) for the activities she performed.